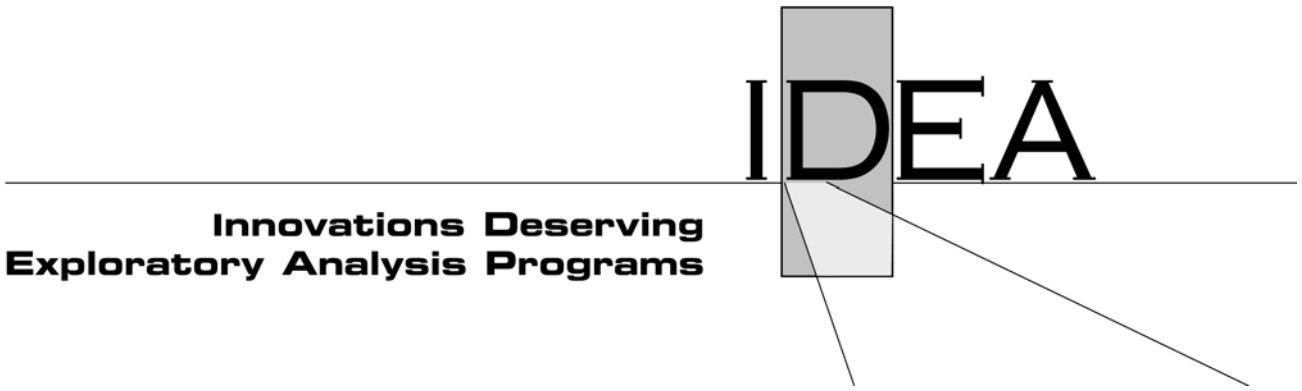

Intelligent Technology System Program

A Mobile Road Condition Sensor as Winter Maintenance Aid

Final Report for ITS-IDEA Project 85

Prakash Joshi, Physical Sciences, Inc.

May 2002

TRANSPORTATION RESEARCH BOARD • NATIONAL RESEARCH COUNCIL

Acknowledgement: This project was funded by Contract No. ITS-85 issued by the National Academy of Sciences under the Department of Transportation Agreement No. DTFH61-92-X-00026.

The information provided herein is not to be relied upon for the development or production of instrumentation. This report is not necessarily accepted by the Academy of Sciences or by the Federal Highway Administration, nor does the Academy or the Federal Highway Administration necessarily accept the findings, conclusions, or recommendations either inferred or specifically expressed herein.

TABLE OF CONTENTS

LIST OF FIGURES

LIST OF FIGURES (Continued)

EXECUTIVE SUMMARY

The knowledge of the presence of ice, water, snow, and other substances on road surfaces is essential for a number of reasons. Maintenance vehicles need this information to determine the type and extent of surface treatments needed for keeping roadways drivable. These substances can seriously degrade the traction between the tires and road surfaces, resulting in hazardous driving conditions for automobiles and trucks. Thus information on road condition, especially when it is not readily apparent to the operator (e.g., black ice), can be used to alert the driver to slow down and maintain vehicle control. Apart from this need for vehicle-mounted road surface characterization, there are other applications of ice/snow/water accumulation information, such as triggers for signs warning motorists of icing on bridges, control inputs for timing of yellow/green lights at intersections, and for control of vehicular traffic as part of Intelligent Transportation Systems (ITS). Physical Sciences Inc. (PSI) conducted a Type 1 (ITS-50) study to determine the feasibility of developing a vehicle-mounted device for sensing the presence of ice/water and other materials on pavement surfaces and developed an engineering prototype of the device under the program ITS-85. This report describes the results of the latter program.

We have investigated and developed a compact, lightweight, vehicle-mounted sensor system based on backscatter of infrared radiation (emitted by an onboard light source) from the road surface. The development of such a device has now become practical and potentially affordable on a commercial scale due to technological advances, simultaneously with lower costs, in electronics including high performance, inexpensive microcontrollers, uncooled IR detectors, and fiber optics. Our sensor system is designed to detect and continuously monitor films and layers of ice, water, snow, sand and other substances on asphalt and concrete pavement surfaces. The detected signals are processed in real time by an onboard microprocessor and displayed graphically on a laptop PC screen as a user-friendly, informative map for the vehicle operator. The prototype sensor and its electronics are packaged into a rugged, compact, and lightweight device that can be mounted on a truck or a maintenance vehicle. Careful measurements have been performed at the Cold Regions Research and Engineering Laboratory (CRREL) to calibrate the sensor for films and layers of water, ice, dry and wet snow, sand and various mixtures over asphalt surfaces. CRREL mounted the prototype sensor on their Instrumented Research Vehicle (IRV) and conducted tests on wet, icy, and snow-layered roads during winter in New Hampshire. Simultaneous measurements of vehicle traction were also made by CRREL in these tests. Additional winter tests at low speeds were conducted by PSI where the device was mounted on a Massachusetts Highway Department pick-up truck and by the Colorado Department of Transportation on a winter road maintenance vehicle. The data from all tests clearly demonstrate the ability of the prototype device to characterize and discriminate among various road conditions. This report describes the design and development of the prototype road condition sensor system, its calibration, and field testing under the IDEA program.

1. INTRODUCTION

The knowledge of the presence of ice, water, snow, and other substances on road surfaces is essential for a number of reasons. Maintenance vehicles need this information to determine the type and extent of surface treatments (e.g., NaCl or $CaCl_2$ and the amount to be sprayed) needed for keeping roadways drivable. These substances can seriously degrade the traction between the tires and road surfaces, resulting in hazardous driving conditions for automobiles and trucks. This information on road condition, especially when it is not readily apparent to the operator (e.g., black ice), can be used to alert the driver to slow down and maintain vehicle control. Apart from this need for vehicle-mounted road surface characterization, there are other applications of ice/snow/water accumulation information, such as triggers for signs warning motorists of icing on bridges, control inputs for timing of yellow/green lights at intersections, and for control of vehicular traffic as part of Intelligent Transportation Systems (ITS).[1] Physical Sciences Inc. (PSI) conducted a Type 1 (ITS-50) study to determine the feasibility of developing a vehicle-mounted device for sensing the presence of ice/water and other materials on pavement surfaces. The results of this work are described in Reference 2. This report describes the development of an engineering prototype of the device under the program ITS-85.

The present state-of-the-art of determining the presence of surface contaminants on pavements includes remote infrared (IR) surface temperature sensors mounted on maintenance vehicles, *in-situ* deicing chemical sensors embedded in roadways, and passive ice/water sensors mounted alongside the road based on backscatter of sunlight from the road surface. The research reported here investigated a compact, lightweight, vehicle-mounted sensor based on IR backscatter of radiation emitted by an onboard light source from the road surface. The development of such a device has now become practical and potentially affordable on a commercial scale due to technological advances, simultaneously with lower costs, in a number of areas. These include very compact solid-state diode lasers; near-coherent Light Emitting Diodes (LEDs); uncooled, solid state IR detectors, such as germanium and indium-gallium-arsenide; high performance, inexpensive microcontrollers; highly miniaturized low-cost electronics; and fiber optics. This report describes our work on the development of a prototype road condition sensor system, its calibration, and field testing.

The problem of monitoring road surfaces for icy/wet conditions has received considerable attention over the years.[3-5] In recent years, advances in sensor technologies have been employed to detect and measure the accumulated ice/water layers on surfaces. For example, PSI's prior work for the U.S. Army[3] demonstrated the feasibility of detection of ice using a 3 μm infrared laser beacon. This work was further advanced under PSI's IR&D program by making the measurements in the infrared at two near infrared wavelengths and correlating the ratio of intensities at these wavelengths to the thickness of water, and ice-water layers on a surface.

In this report we describe the work performed under the ITS-IDEA program to detect films of ice, water, snow and other substances on asphalt and concrete pavement surfaces. Our technique employs optical detectors in the infrared, optical fibers, and integrated processing electronics. The prototype sensor and its electronics are packaged into a rugged, compact, and lightweight device that can be mounted on a truck or a maintenance vehicle. Careful measurements have been performed at the Cold Regions Research and Engineering Laboratory (CRREL) to calibrate the sensor for films and layers of water, ice, dry and wet snow, sand and various mixtures over asphalt surfaces. CRREL mounted the prototype sensor on their Instrumented Research Vehicle (IRV) and conducted tests on wet, icy, and snow-layered roads during winter in New Hampshire. Simultaneous measurements of vehicle traction were also made by CRREL in these tests. Additional winter tests at low speeds were conducted by PSI where the device was mounted on a Massachusetts Highway Department pick-up truck and by the Colorado Department of Transportation on a winter road maintenance vehicle. The data from all tests clearly demonstrate the ability of our device to characterize various road conditions to discriminate among these substances as distinct from a dry or moist pavement. We have thus demonstrated that the mobile sensor technology developed under this IDEA program provides accurate and continuous measurement of road conditions directly underneath the vehicle.

2. TECHNICAL OBJECTIVES

The overall objective of this project was to develop and demonstrate in the field an engineering prototype of a vehicle-mounted road surface condition sensor system capable of detecting, characterizing, and discriminating the presence of thin layers of ice, water, snow, sand, and other substances in real time using optical spectroscopic techniques.

A concurrent objective was to ensure that the design and construction of the sensor system resulted in a low cost device that could be transitioned to a commercial product.

The specific objectives of this program were to:

1. Develop a compact mechanical design of the sensor system addressing operation in cold winter conditions, sensor surface obscuration by ice films and/or dirt layers, and various solar conditions.

2. Develop an electro-optical design of the sensor system for high signal-to-noise ratio, high road surface sampling rates, and fast on-board data processing using inexpensive commercial processors.

3. Develop discrimination algorithms to characterize the road surface conditions and develop a user-friendly road condition display interface.

4. Fabricate and assemble sensor system and characterize in the laboratory

5. Conduct environmental testing and field testing under winter conditions.

6. Work with a commercial company to transition the prototype device to a potential product.

3. DESIGN AND FABRICATION OF ENGINEERING PROTOTYPE SENSOR SYSTEM

3.1 BACKGROUND

The scientific principles underlying the road condition sensor for detection and spectral characterization of ice, water, and other substances have been described in detail in the final report of our Type I IDEA project ITS-50.[2] Under the ITS-50 project a breadboard prototype sensor was developed and the feasibility of our optical sensing technique was demonstrated. We summarize below the results of the Type I project to provide the context for further developments of an engineering prototype under the current ITS-85 project.

PSI completed a Type I Concept Exploration investigation that established the feasibility of detecting thin films of ice, snow, water, and ice-water mixture on road surfaces using an optical spectroscopic technique. The schematic of our detection concept, shown in Figure 1, involves illumination of the road surface with a broadband light source and measurement of diffused reflection from the road surface in three wavelengths with filtered detectors. The ratios of measured intensities at the three infrared wavelengths (λ_1, λ_2, and λ_3) and the changes in absolute values of individual intensities provide unique discrimination among ice, snow, water, and ice-water mixtures as well as sand layers and moist and dry pavement surfaces.

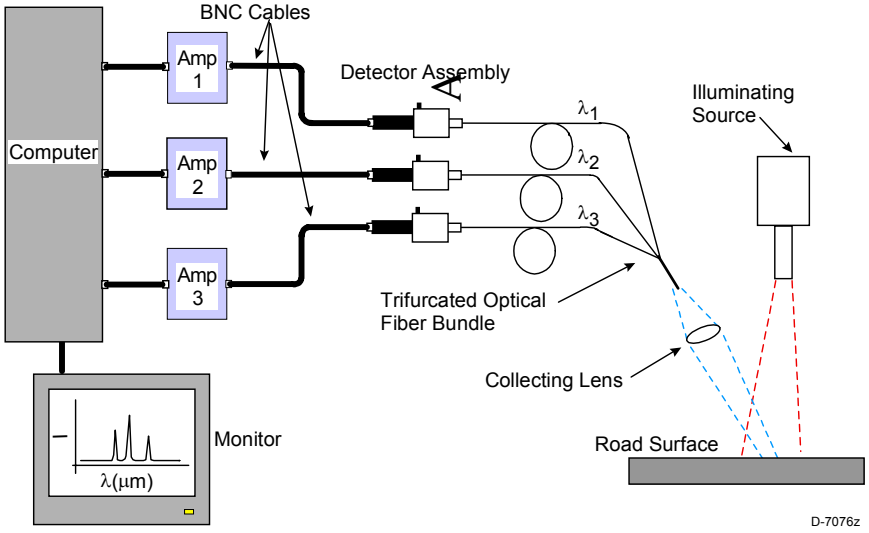

FIGURE 1 Schematic of sensor system developed in Type I project.

In Figure 1, the light source is typically about 50 cm above the road surface and the spot illuminated on the road measures approximately 35 mm in diameter. The three wavelength signals were sampled at 400 Hz to 1 kHz. At these rates, the spot on the ground would translate less than 30 to 75 mm between samples at a vehicle speed of 100 km/h. The signals can be averaged to characterize the pavement over an appropriate distance, for example, one vehicle length.

We fabricated a proof-of-concept laboratory sensor system and a breadboard prototype sensor system during the Type I project. Sensor responses were characterized in the laboratory during transition of thin layers of ice and snow to

water to demonstrate the feasibility of the detection scheme. Preliminary low speed tests of the vehicle-mounted prototype were also conducted to characterize sensor response on asphalt with layers of ice, snow, water and sand. We present some examples of the low speed test data to illustrate the feasibility of our spectroscopic sensing technique.

3.1.1 Traverse Over Ice Followed by Dry Region

Figure 2 illustrates measurements obtained during traverse over an icy region followed by dry pavement. The raw sensor data in the three detector channels sampled at 1 kHz are shown in Figure 2(a). Over the dry surface, the detector current in all channels increases, with a much reduced spread among the three channels. We also see clearly the presence of white lines in the parking lot where the tests were conducted. These lines are characterized by large increases in all detector channels due to high reflection from the white paint. The data in Figure 2(a) were smoothed using an 8-point moving average and the averaged data were ratioed and plotted in Figure 2(b). The λ_2/λ_3 detector current ratio stands out over the icy region whereas the λ_2/λ_1 ratio is flat over that region. The λ_3/λ_1 current ratio is nearly the inverse of the λ_2/λ_3 data. Most importantly, beyond the icy region, the ratios are essentially flat and all the noise in the individual detector channels is "cancelled out". This test clearly demonstrates the ability of our sensing scheme to isolate icy regions of the pavement.

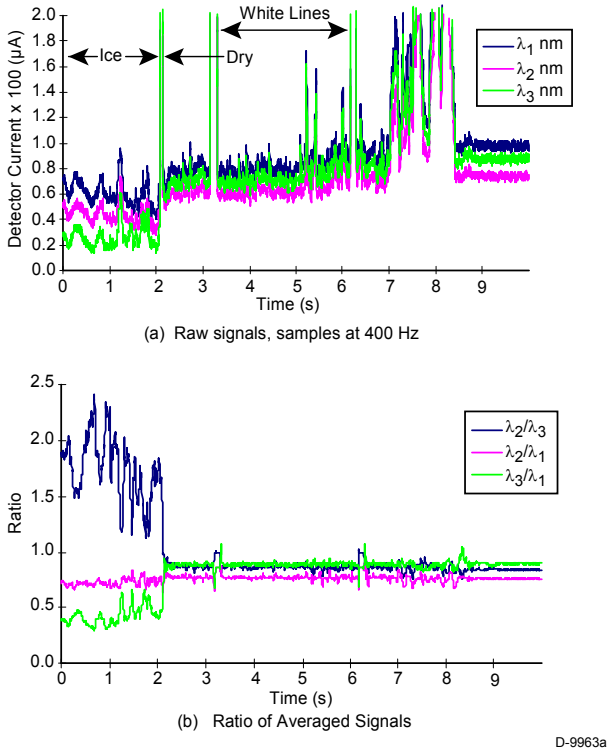

FIGURE 2 Sensor response during traverse over an icy region followed by a dry region.

3.1.2 Traverse Over Water-Ice Mixture Followed by a Sandy Region with a Narrow Ice Patch

In one of our tests we simulated the realistic situation of winter conditions of water over ice and a sandy region. A narrow ice patch, fortuitously present on the pavement, provided a test of the ability of our technique to pick out ice. Over the water-ice mixture, Figure 3(a), we see trends in detector outputs similar to the icy regions in the previous case (Figure 2), except that the λ_2 channel current is depressed to a greater degree. We observe this behavior consistently whenever water is present and it is reflected in the ratio data, Figure 3(b). Again, the icy region is indicated by significantly high values of the λ_2/λ_3 current ratio, but in addition, the presence of water is indicated by a significant reduction in the λ_2/λ_1 ratio. Beyond the water-ice region, the ratios stay essentially flat, with the clearly noticeable exception of the ice patch accompanied by a sharp rise in the λ_2/λ_3 ratio. We did not characterize this patch sufficiently to know whether water was also present in the patch, which would have explained the simultaneous drop in the λ_2/λ_1 ratio. It is worth noting from the averaged signal data, Figure 3(a), that over the sandy region all channels exhibit significant increase in detector current due to scattering from the sand. However, this effect is hidden in the ratio data of Figure 3(b).

3.1.3 Traverse Over a Water Layer Followed by a Dry Pavement

This test was similar to the previous test, but a with a thin layer of pooled water (~1 mm) followed by dry pavement. The data are shown in Figure 4. It is seen that the λ_2/λ_3 ratio remains flat and the λ_2/λ_1 ratio decreases significantly when moving from a dry to wet pavement.

3.1.4 Traverse Over Moist Regions Separated by Packed Snow

The averaged data in Figure 5(a) show increased signals in the λ_1 and λ_2 nm channels due to scattering, when moving from moist pavement to snow-covered pavement. The λ_3 nm signal decreases in magnitude. The ratio data, Figure 5(b), show a more consistent, high value (average ~4) of the λ_2/λ_3 ratio over the snow region. There is also a decrease in the λ_2/λ_1 ratio as in the last test. All ratios are flat, ~0.8 to 1, over the moist region.

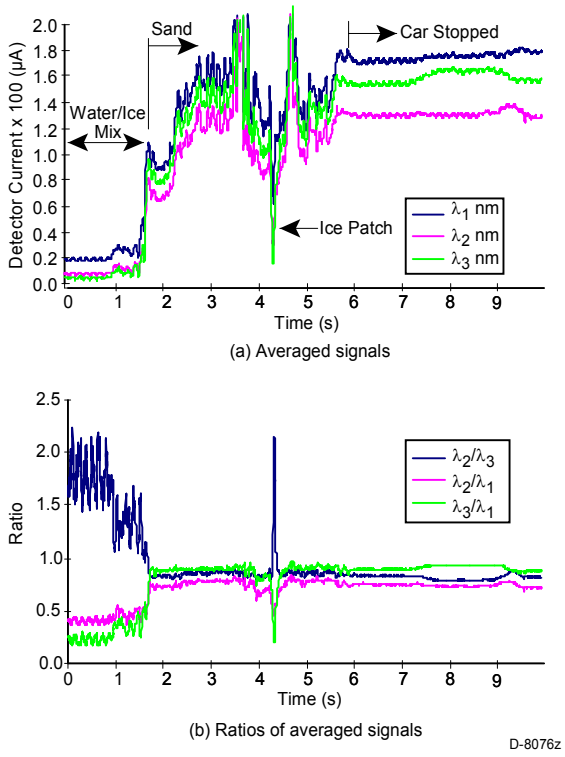

FIGURE 3 Sensor response during traverse over a water-ice mixture region followed by a sandy region containing a narrow patch of ice.

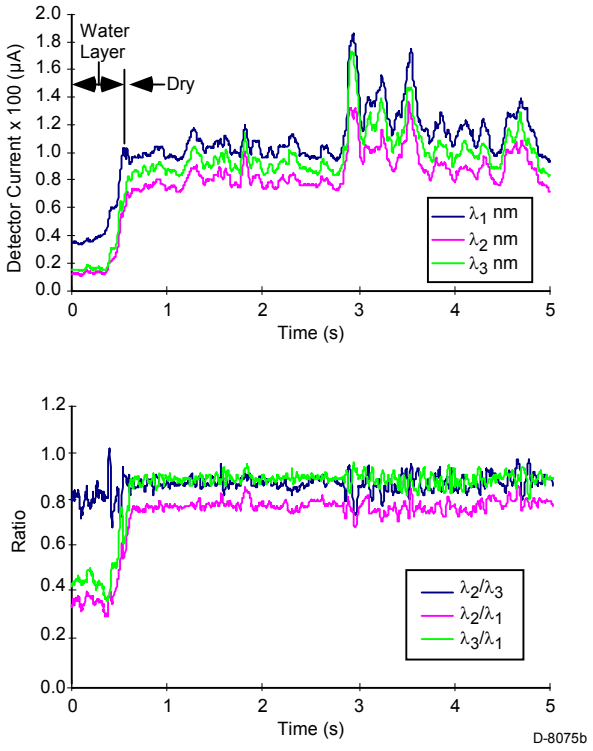

FIGURE 4 Sensor response during traverse over a water layer followed by a dry pavement.

The preceding discussion clearly demonstrates that the ability of our sensor to characterize the pavement condition using the near-IR optical sensing technique. From the measurements of changes in the absolute values of the signals in the three wavelength channels (relative to dry or moist pavement), the ratio of the signal in the λ_2 channel to the signal in the λ_3 channel, and to a lesser extent, the ratio of the signal in the λ_2 channel to the signal in the channel, we discriminate among ice, snow, water, ice-water mixture, and sand layers on pavement. In Table 1, we summarize the magnitudes of ratios of signals at λ_2 to λ_3 (R_{λ_2/λ_3}) and λ_2 to λ_1 (R_{λ_2/λ_1}) channels for discriminating among various layers. Also included in the table is the absolute value of the signal in the λ_1 channel normalized by its magnitude over the dry pavement ($\hat{S}$). $\hat{S}$ allows discrimination between dry, noise, and sandy surfaces. It is seen that the λ_2 to λ_3 signal ratio is clearly a sensitive indicator of ice and snow. During the present project, we conducted extensive field and laboratory tests to validate the data in Table 1 and the results were incorporated into algorithms that enable real-time, microprocessor-based decisions on pavement surface condition.

3.2 SENSOR SYSTEM DESIGN

The design philosophy for the sensor was as follows:

- Simple, reliable, user-friendly design
- A well-engineered prototype instrument
  - demonstration of all functions of a potential commercial product
  - ice, water film detection and discrimination as well as other different types of road surface conditions such as sand, snow, dry, moist, etc.
- Accurate calibrations at CRREL facility
- Operation under different winter weather and solar illumination conditions
- Operation and survival under platform vibration and EMI environment

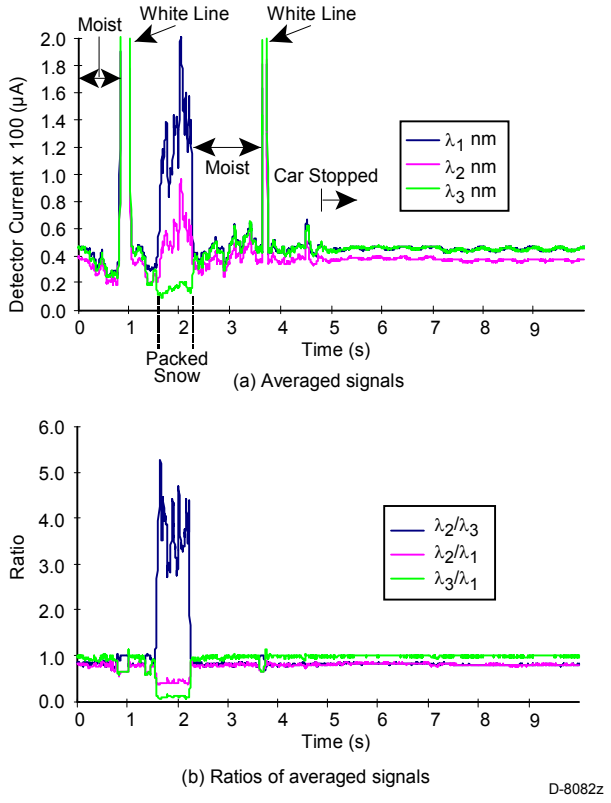

FIGURE 5. Sensor response during traverse over moist regions separated by packed snow.

TABLE 1 Variation in Ratios of Wavelengths in λ_2 to λ_3 and λ_2 to λ_1 Signals Results from Type 1 Project

Pavement Layer/ Condition	R_{λ_2/λ_3}	R_{λ_2/λ_1}	$\hat{S}_{\lambda_1}$
Ice	≥ 1.5	< 0.8	0.45→0.70
Snow	≥ 3	< 0.5	1.4 →2.0
Water	~ 0.8	< 0.5	0.2/0.25
Sand	0.8 to 1	< 0.8	1.6 to 1.7
Moist	0.8 to 1	< 0.8	0.40
Dry	~ 0.8	0.7 to 0.8	1.0

- Operation in presence of surface treatments, water spray, contaminant deposition
  - minimize false indications
- Prototype design substantially same as a potential commercial product
  - geometric envelope, weight, power, electrical and display interfaces with a host vehicle
    - mechanical mounting to depend on host vehicle
  - prototype to include extra diagnostic features
- Prototype sensor components (electro-optical) and fabrication
  - as low cost as possible
  - design/parts selection not optimized for lowest cost resulting from economies of scale, which will be a consideration for commercial product.

Some specific technical issues resulting from breadboard developments of the Type I project (Reference 2) were also addressed during the design stage. These issues are listed in Table 2, along with the solutions and improvements incorporated during the current project.

TABLE 2. Design Solutions and Improvements Addressing Technical Issues from Type 1 Project Breadboard Prototype Development

Issue	Solution/Improvement
• Degraded S/N ratio at low sun angles (winter, high latitudes)	– Higher light source intensity (75 W) – Photodiode to correct for solar reflectance from pavement
• Effects of condensation and dirt/salt deposition on optics	– Heated glass cover in front of optics · startup procedure, initial warmup – Forced air flow over glass cover · sensor mockup tests – Periodic optical calibration, indicating glass cover needs cleaning
• Effects of water and mud spray on optics	– Mud flaps in front and on sides of sensor housing – Forced air flow over glass cover · sensor mockup tests
• Sensor maintainability	– Simple mechanical/electrical interfaces with host vehicle – Sensor cleaning (low signal) warning light
• Sensor location on vehicle for least contamination effects and view of road away from tires	– Locate sensor behind front bumper, between wheels, behind radiator
• Mechanical ruggedness of packaging	– Choice of materials, design, extensive vibration testing

Figure 6 shows a block diagram of the mechanical system design implementation of the sensor system schematic shown in Figure 1. The sensor assembly is divided into two compartments, optics and electronics. The optics compartment houses the light source, collection optics, optical fiber bundles, a part of each sensor/preamplifier assembly, and a small mirror assembly within path of the fiber for the λ_1 channel. This "cold" mirror reflects visible portion of the light into a photodiode and the NIR portion into the λ_1 filter/detector. The measurement of visible light intensity will be used to correct for the effects of solar reflectance from the pavement on readings in the λ_1 and λ_3 channels relative to the λ_2 channel. The optics compartment also includes a quartz window, a resistance heater for the window and a power relay for the heater, and a fan for blowing air externally over the glass to keep it clean from dirt. (We found during our field testing that the fan was actually unnecessary, at least for the host vehicle configurations used in the tests.) The electronics compartment incorporates two circuit boards, a power board which houses power supplies and a processor board which houses a microprocessor, communications and peripheral electronics as well as a photodiode for the measuring solar reflectance. The system operates on 12V supply from the vehicle's automotive battery.

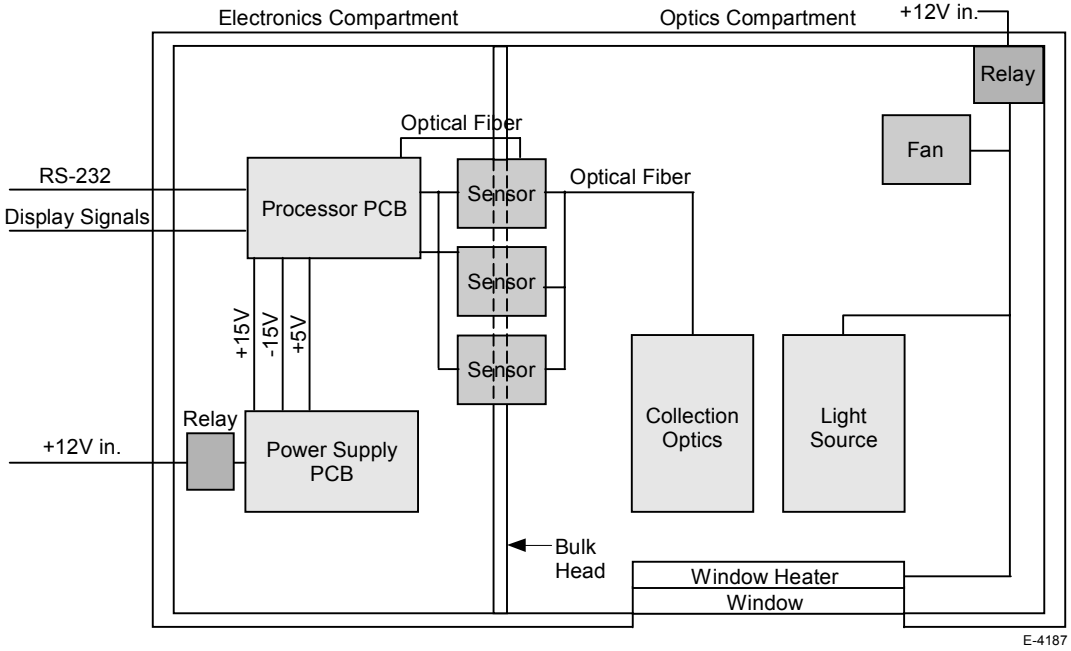

FIGURE 6 System mechanical block diagram.

A three-dimensional perspective of the interior of the sensor is shown in Figure 7. It illustrates the mounting of the electronics boards on front and back walls of the electronics compartment. Also shown are the mirror assembly for solar photodiode in the optics compartment, the sensor window, light source, light collection optics assembly, fiber bundles, and three filter/detector assemblies. The front and rear views of the sensor are shown in Figure 8. (If needed, a flexible mudflap will be installed around the sensor box to prevent splashing of water, snow and dirt on the window.) The sensor weight is approximately 10 kg.

Figure 9 shows schematically the mounting of the sensor prototype on a vehicle (e.g., a pickup truck from Massachusetts Highway Department or the Instrumented Research Vehicle from the Cold Regions Research and Engineering Laboratory, CRREL). For initial road testing of the instrument, we envisioned two individuals in the vehicle, the driver and an experimenter. The experimenter operates the instrument (on/off), initiate data acquisition and make visual observations of the road surface. The figure shows two displays, one for the driver indicating the road condition as interpreted by the sensor and a second display which is part of the experimenter's laptop computer. For purposes of prototype tests, we simply used the computer display. As the sensor became well characterized, the data acquisition operation became simpler, and only one person, the driver, was able to perform all operations.

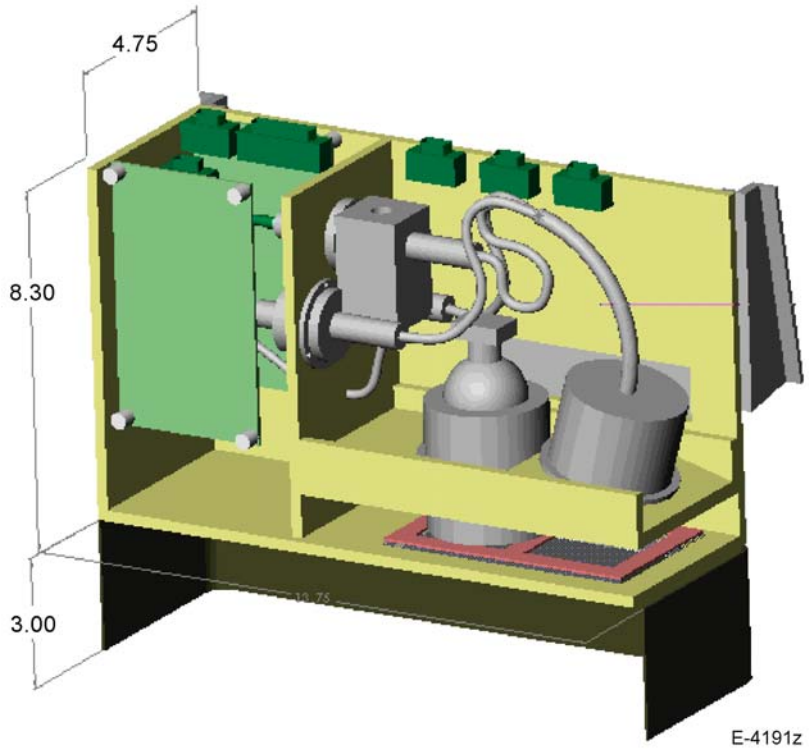

FIGURE 7 Interior view of prototype sensor.

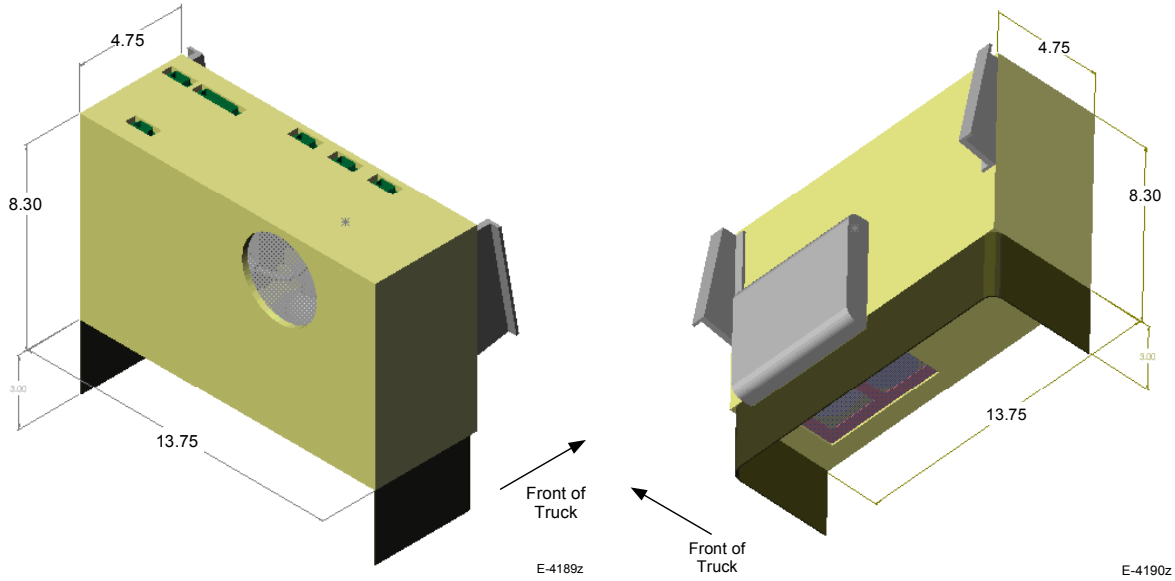

(a) Front View (b) Rear View

FIGURE 8 Front and rear views of sensor prototype.

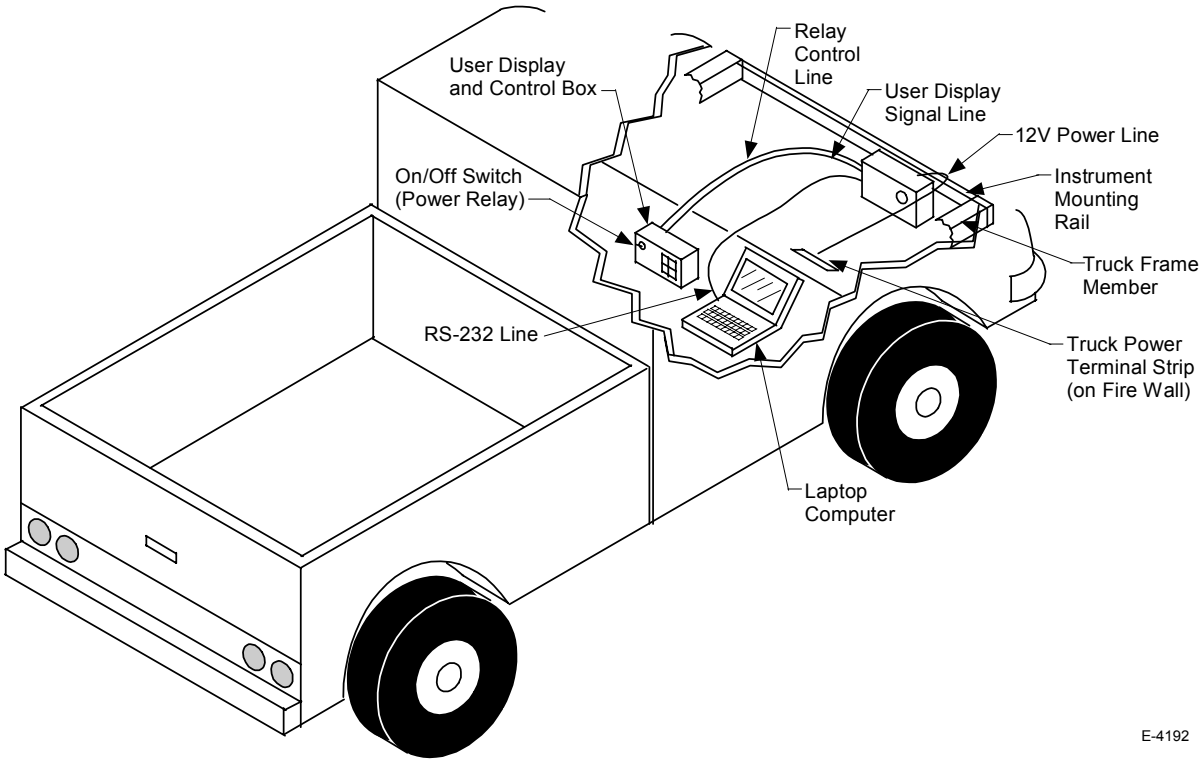

FIGURE 9 Prototype mounting and road sensor configuration.

Figure 10 shows our approach to the development of a computer display of road condition information as sensed by the instrument. It shows a map of the averaged ice-snow indicator ratio (R_{is}) as a function of the wetness indicator ratio (R_w) where the ratios are defined by

$$R_{is} = I_{\lambda_2} / I_{\lambda_3}$$

and

$$R_w = I_{\lambda_2} / I_{\lambda_1}$$

where I_{λ_1}, I_{λ_2}, and I_{λ_3} are the light intensities (or equivalently, currents) in the three wavelength (or equivalently, detector) channels, λ_1, λ_2, and λ_3, respectively, averaged over at least one car length. The display is refreshed every quarter of a second. The x-axis in Figure 6 represents a range from very wet (or a thin layer of standing water) to very dry pavement. The y-axis represents the density of the contaminant, from higher density (water) to lower density (ice) to lowest density (fluffy snow). Using this physical interpretation the map of Figure 10 will be divided into various regions (wet, moist, day, ice, snow, slush, etc.). The boundaries delineating the regions will be diffuse (i.e., overlapping regions) in reality and not as distinct as shown in Figure 10.

Figure 11 shows the functional block diagram of the sensor system including electronics. 12 V power from the vehicle battery is conditioned to produce 5 V and ±15 V power for the processing electronics. Unconditioned 12 V power is used for the fan, illuminating lamp, and the resistive heaters. Signals from the three NIR detector amplifiers, the reflected (from the road surface) solar intensity photodetector as well as an (optional) window temperature sensor are processed by the microcontroller. The signals are appropriately averaged and the light intensity ratios for the three bands are computed and averaged (typically over one car length at 30 mph). The microcontroller also controls the operator visual display and the RS-232 communications with the laptop computer. The power estimate for the sensor, including electronics, is less that 90 W. This includes a 75 W light source, a 10 W window heater and a 5 W fan.

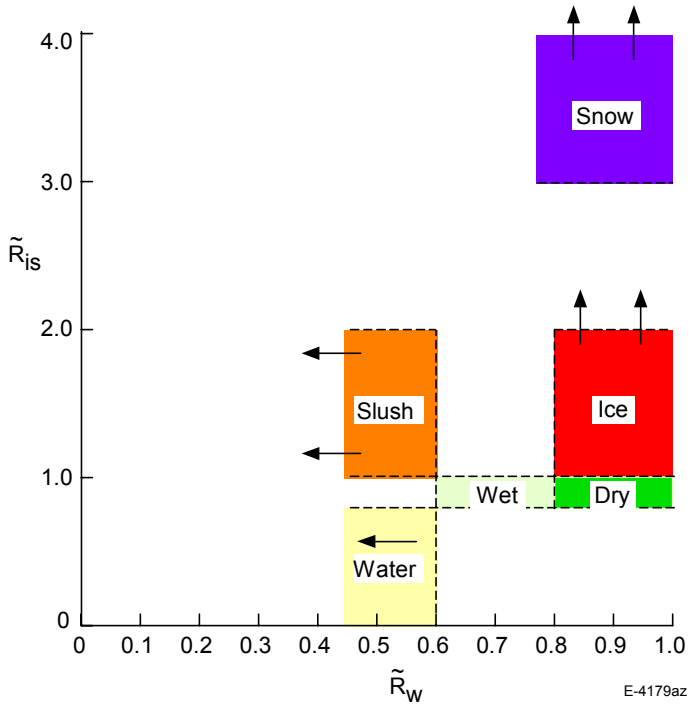

FIGURE 10 Approach to comprehensive road condition indicator display.

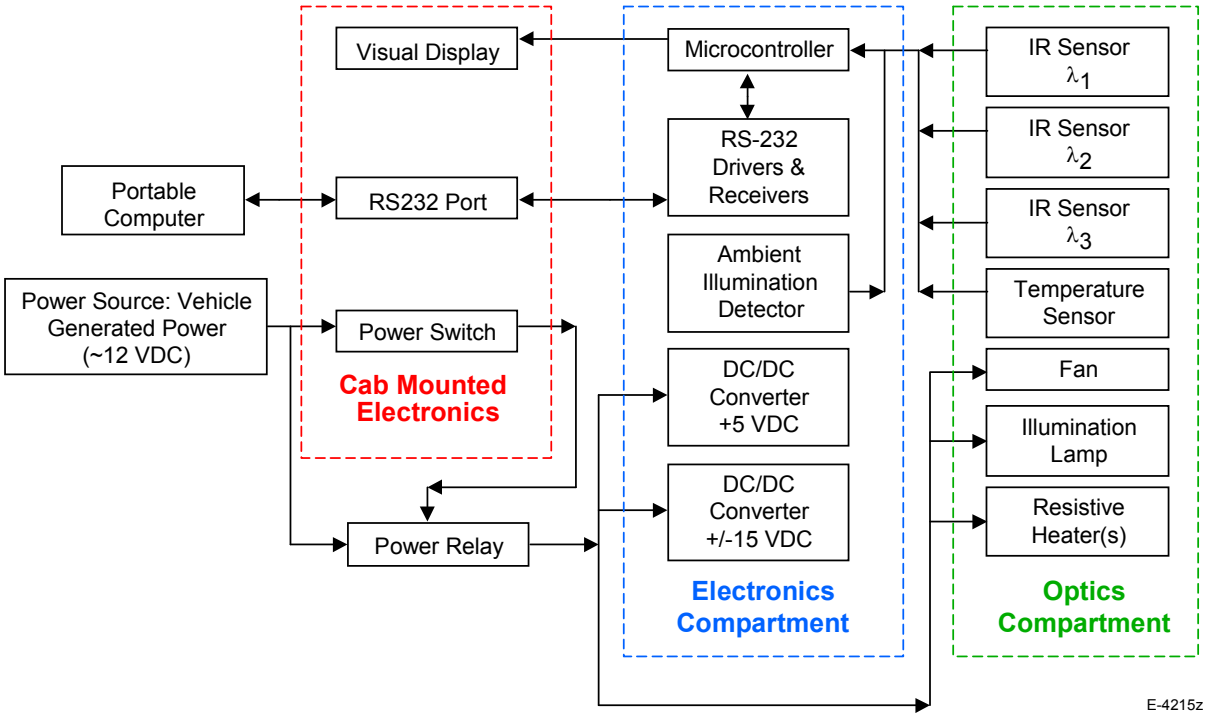

FIGUER 11 Functional block diagram of sensor system.

We performed extensive thermal analyses of the window that protects the sensor optics (Figures 6, 7, and 8). A typical calculation is shown in Figure 12 for cooling by 25 mph airflow (due to the fan) with the ambient temperature at –10°C. With the 10 W heater operating, it is seen that the window stays quite warm, the lowest temperature being about 12°C.

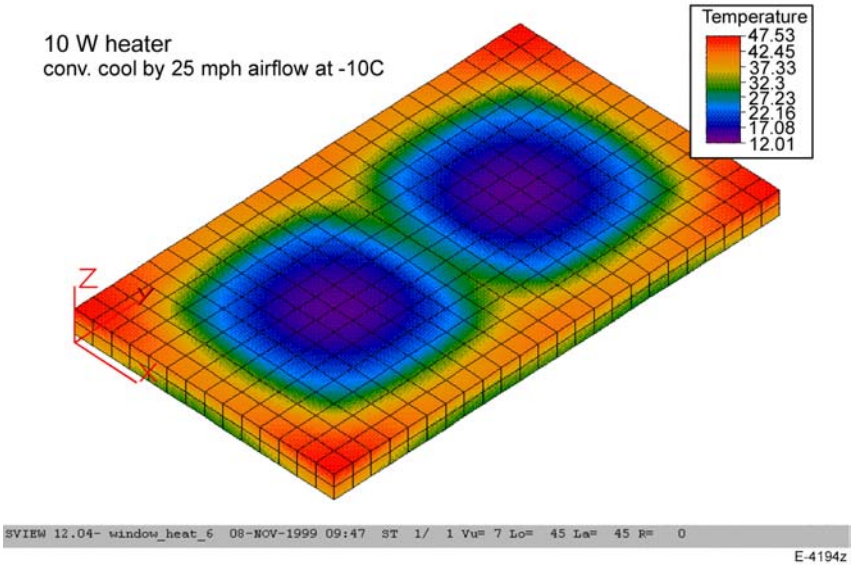

FIGURE 12 Results of finite element thermal model of sensor window.

The sensor system design presented above was reviewed by a panel of experts listed in Appendix A. Following this review, fabrication of the sensor system was initiated.

3.3 FABRICATION

In keeping with the design philosophy discussed above, we selected commercial off-the-shelf optics, electronics, and mechanical components for fabrication. The key optical components were a broadband VIS-NIR light source, a trifurcated optical fiber, narrow band optical filters with center wavelengths λ_1, λ_2, and λ_3 nm, and integrated detectors/amplifiers. Other optical components included various collimating and focusing lenses, a cold mirror, and a silicon photodetector. Key electronic components were an inexpensive but versatile microcontroller (with communication chips), DC-DC converters, power relays, a window heater, and water-tight connectors. Key mechanical components included the viewing window, a compact fan, structural housing, and mounting brackets.

The optical components represent the most significant cost element for the instrument and we worked with vendors to meet our requirements at the lowest possible prices. Electronics board layouts were produced at PSI and an outside vendor fabricated the boards. Software for the processor was developed at PSI for signal averaging, computing intensity ratios for the three wavelength channels, and packaging digital data for transmission to a laptop computer. The housings for optical components were fabricated at PSI. The optical system was assembled at PSI and tested for alignments, throughputs, noise characterization, and signal-to-noise determination. The mechanical housing was fabricated partly at vendor facilities and partly at PSI. The complete instrument prototype was assembled at PSI. Basic functionality tests of the optics and electronics were conducted.

Figure 13 shows photographs of the instrument. Figure 13a shows the bottom view. The light source and collector assemblies are seen through the quartz window. The brackets on the housing were designed for mounting to the underside of a pickup truck provided by the Massachusetts Highways Department. Figure 13a also shows the fan intake, seen more clearly in the back view of the instrument in Figure 13b. The interior of the instrument is shown in the front view of Figure 13c, where the cover plates for the optics and electronics compartments have been removed. In the optics

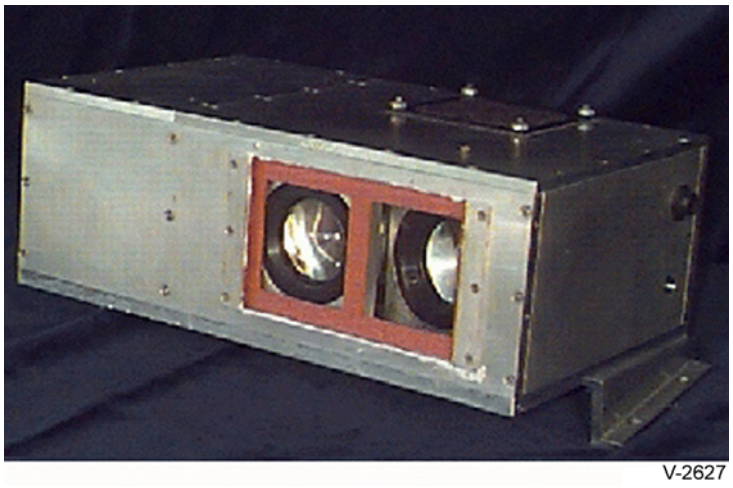

(a) Bottom View

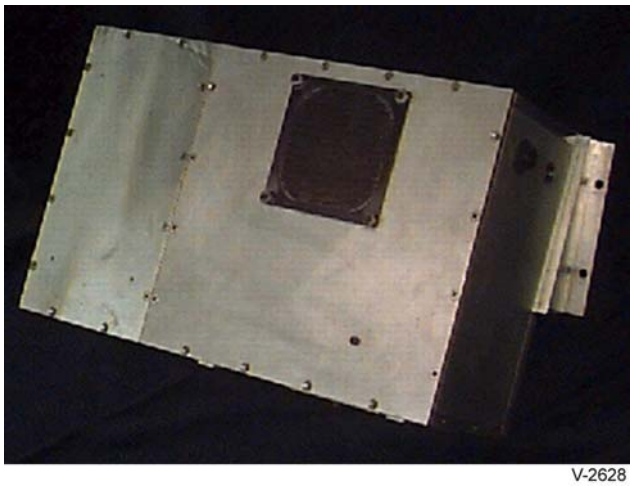

(b) Back View

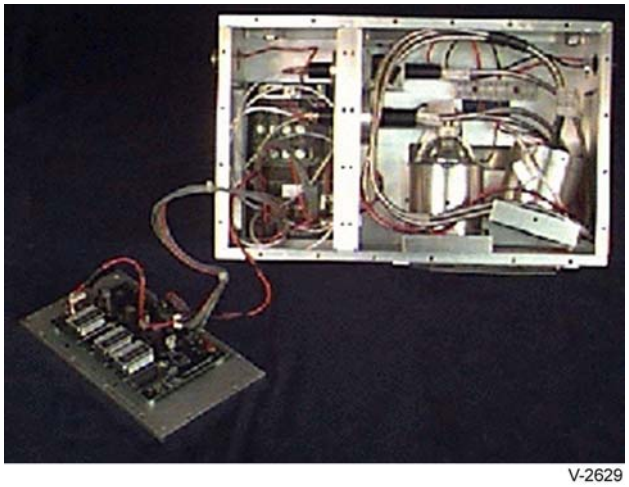

(c) Interior View

FIGURE 13 Photographs of road condition sensor instrument prototype.

compartment on the right, we see the light source assembly fastened normal to the window and the collector assembly (on a movable fixture, not seen in the photograph) that can be adjusted to provide the desired alignment. Note the exit of the fan underneath the optics compartment. This view also shows the optical fiber and filter/detector assemblies. The electronics compartment on the left shows the detector/amplifier assemblies and the processor board on the back wall. The power board is mounted behind the front cover as shown on the bottom left of the view in Figure 13c.

4. TESTING AND CALIBRATION OF SENSOR SYSTEM

4.1 INSTRUMENT SHAKEDOWN TESTS

The first set of tests on the prototype instrument was conducted on a Massachusetts Highways Department pickup truck. These tests were performed during typical winter conditions in Andover, Massachusetts on paved roadways in the vicinity of PSI facilities. The purpose of these shakedown tests was to evaluate:

- Physical integrity of the instrument in the vibration and shock environment during normal winter driving conditions (e.g., ambient environment and road conditions).
- Robustness of the mounting arrangement (brackets, fixtures, and fasteners) on the particular maintenance vehicle.
- Effects of automobile power supply fluctuations during engine start up and operations of other systems (e.g., wipers and radiator cooling fan) on instrument functionality.
- Effectiveness (or the need) for a mud flap around the instrument to prevent splashing of dirt, ice, and snow on the optical window.
- Effectiveness of the fan incorporated in the instrument to maintain constant airflow over the optical window (Figure 6 and 8).
- Accumulation of contaminants on the window during vehicle operation.
- Ease of operating the instrument and acquiring data on the laptop computer for the vehicle operator.
- Quality of sensor signals and processed data.

The brackets in Figure 13b were used to mount the instrument to an aluminum structural beam on the underside of the pickup truck. Figure 14 shows the underside of the vehicle and the mounting holes for the beam. (The beam is not shown.) The bracket angle was designed such that the light was incident at a 10 deg angle relative to the road surface (toward the back of the truck) in order to avoid specular reflection from the road surface into the collector lens.

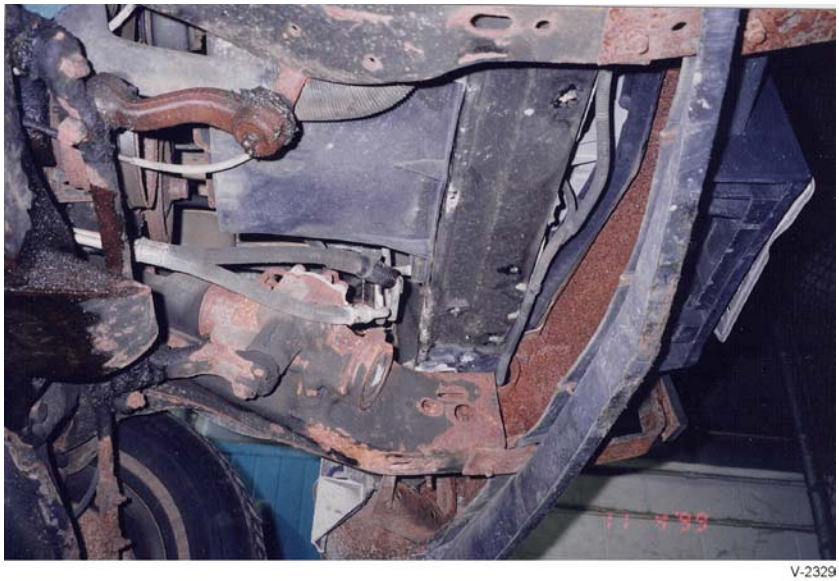

FIGURE 14 Instrument mounting location on Massachusetts Highway Winter Maintenance pickup truck.

The shakedown tests consisted of many "runs" conducted under dry, wet, icy, and snow conditions. We report the following key observations from these tests:

- The instrument maintained its physical integrity during the test. We did not observe any damage to the window or any other subsystems within the instrument when it was opened for inspection.

- We found in early tests that the mounting beam needed additional stiffeners. While the sensor functionality was not affected, the beam was strengthened as a precaution.

- Fluctuations in automotive battery voltage when the wipers were turned on/off had no effect on instrument functionality. The instrument behaved predictably when the ignition was turned on and the data acquisition commenced as expected when commanded by the laptop computer.

- Contrary to our expectation, a mud flap (about 5 inches long) mounted from the front and sides of the instrument actually resulted in accumulation of dirt and snow on the window rather than its prevention. The reason for this was that the flap created an air circulation bubble against the window. This recirculation zone trapped dirt kicked up from the road that eventually coalesced on the surface of the window. We then removed the flap and found that the window stayed clean except for few discrete droplets of water (the window heater was on) that are not expected to affect sensor readings. While window cleanliness will be a function of the location of the instrument in a particular vehicle application, the fact that the flap was not needed in this case is an important result.

- The fan operated continuously upon power up in our tests and there was no accumulation of dirt/snow on the window.

- The shakedown tests were not designed to collect data under controlled road surface conditions (as was the case when we performed calibration tests at the Cold Regions Research and Engineering Laboratory.) The purpose was to obtain sensor signals under realistic field conditions, to ensure that signal intensities are within dynamic range of the system, and to validate the road condition discrimination algorithms. The results from the tests revealed that channels λ_2 and λ_3 are saturated under some conditions, requiring us to incorporate a signal attenuator in front of the collection lens. Some examples of test data are provided below.

Figure 15 shows the data for the gathered by the prototype instrument on mostly dry pavement with some puddles of water. The vehicle speed for this test was approximately 30 mph and signals averaged over approximately one car length are shown in Figure 15a. It is noted that the λ_2 and λ_3 channels become saturated over portions of the pavement. A water puddle, where signal levels in all channels are reduced, clearly stands out. The ratios of intensities in the λ_2 and λ_3 channels and intensities in the λ_2 and λ_1 channels are plotted in Figure 15b. The ratio (R_{is}) of intensity in the λ_2 channel to the intensity in the λ_3 channel is maintained around 0.9 over the dry portion of the pavement. This ratio is significantly lower over pooled water. The ratio of intensity in the λ_2 channel to the intensity in the λ_1 channel (R_w) is around 0.8. This ratio is also significantly lower over pooled water. In Figure 15c, the two intensity ratios R_{is} and R_w are plotted as a map which is divided into various (overlapping) regions of pavement condition. (The rationale and significance of the coordinates of this plot has been explained in connection with Figure 10.) We see that the dry and wet portions of the pavement are clearly discriminated. The points along the ice/dry boundary with R_{is} value identically equal to unity must be ignored in this plot due to the saturation of signal in the λ_2 and λ_3 channels.

Figure 16 shows the test data acquired when the vehicle was driven over a mostly moist region of the pavement with some icy spots. The light intensity signals in the three channels, shown in Figure 16a, appear nominal without any saturation. Although the signals exhibit a significant high frequency content, we observe that the intensity ratios (Figure 16b) are quite clean. When plotted on our road condition discrimination map, Figure 16c, we verify that the instrument indicates the pavement to be mostly wet with few icy and dry regions.

Finally, we show preliminary road test data gathered on a sunny day following a winter storm, Figure 17. In this test, the pavement was quite "messy" with snow, dry, wet, icy, and slushy regions. Again, we see saturation in the λ_3 channel, particularly over snow-covered and some dry regions, Figure 17a. The intensity ratio plot, Figure 17b, shows

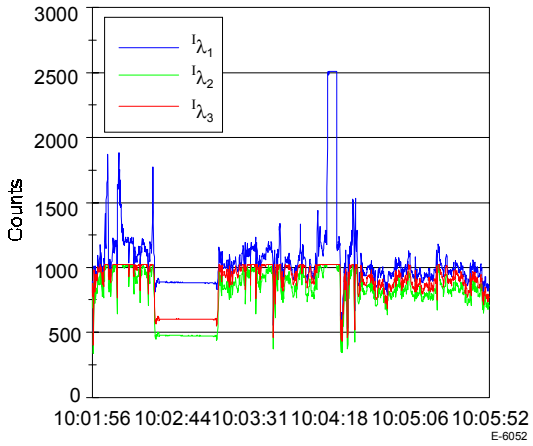

(a) Averaged signals in λ_1, λ_2, and λ_3 channels

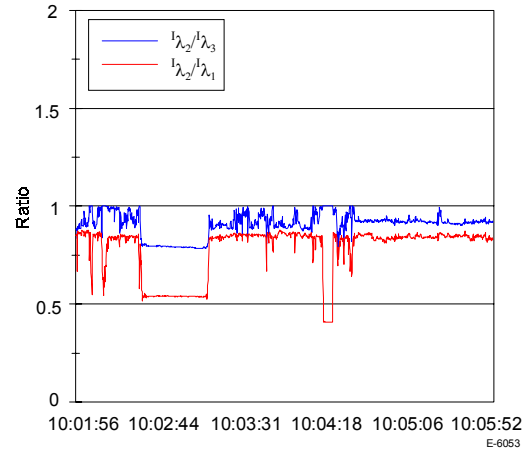

(b) Ratios of intensities in λ_1, λ_2, and λ_3 channels

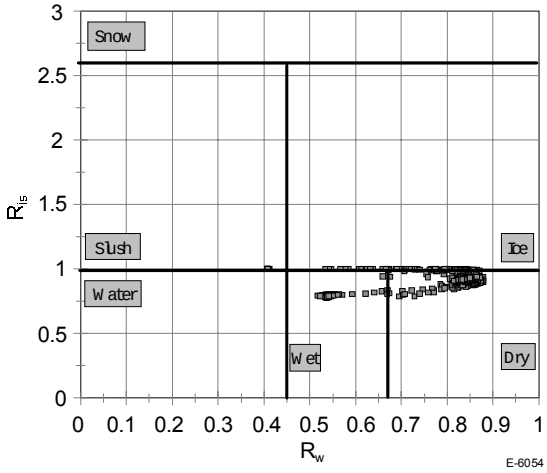

(c) Road condition discrimination map

FIGURE 15 Preliminary road test data on mostly dry pavement with prototype instrument mounted on Massachusetts Highway Department pickup truck.

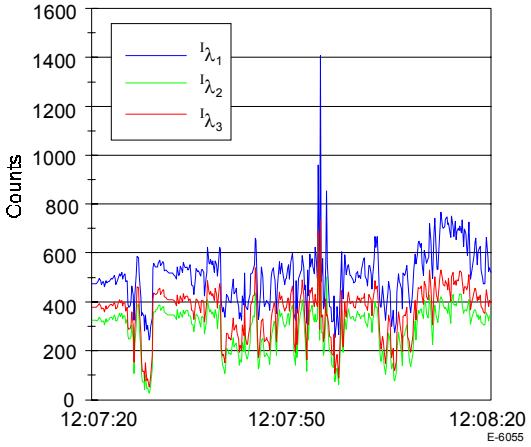

(a) Averaged signals in λ_1, λ_2, and λ_3 channels

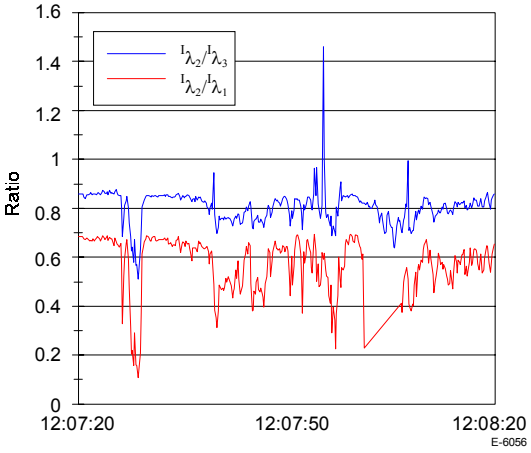

(b) Ratios of intensities in λ_1, λ_2, and λ_3 channels

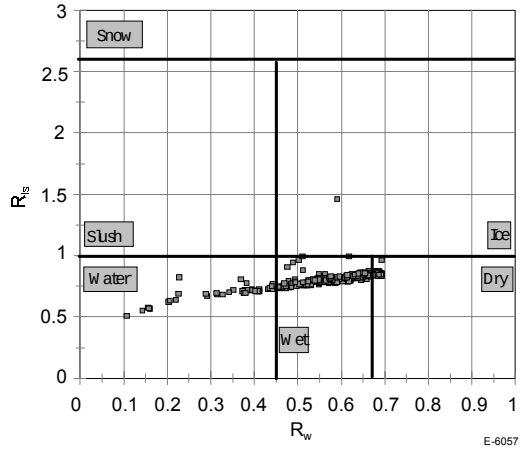

(c) Road condition discrimination map

FIGURE 16 Preliminary road test data on mostly wet pavement with prototype instrument mounted on Massachusetts Highway Department pickup truck.

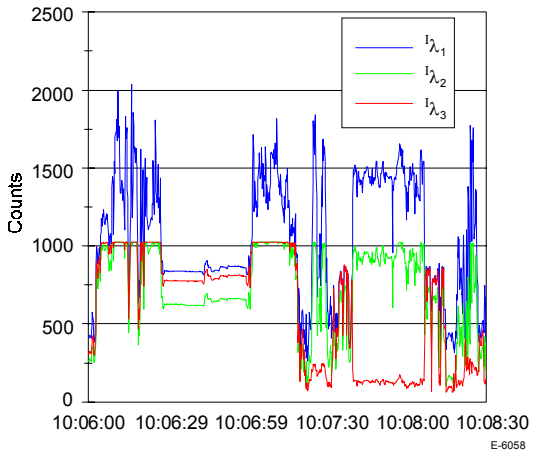

(a) Averaged signals in λ_1, λ_2, and λ_3 channels.

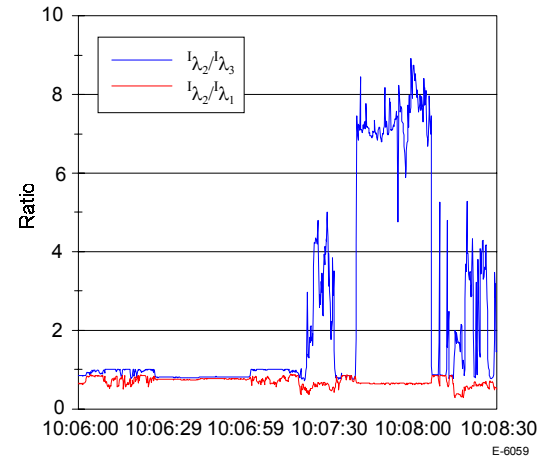

(b) Ratios of intensities in λ_1, λ_2, and λ_3 channels.

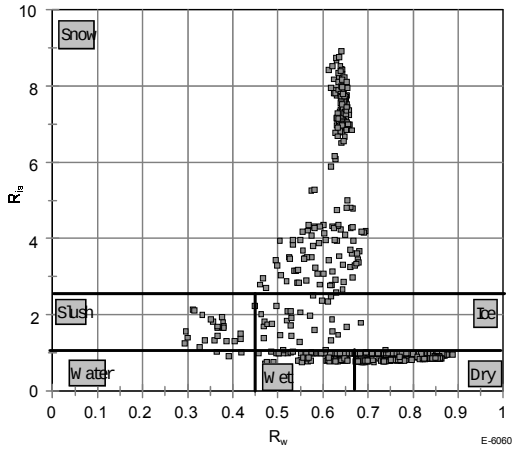

(c) Road condition discrimination map.

FIGURE 17 Preliminary road test data on snow/slush covered pavement with prototype instrument mounted on Massachusetts Highway Department pickup truck.

that the snow and ice regions are clearly differentiated by the instrument. (Again, the points clustered around the ratio R_{is} identically equal to unity are due to saturation of signal in the λ_2 and λ_3 channels and must be ignored.). The discrimination map in Figure 17c gives a snapshot perspective of pavement conditions over the entire region traversed by the vehicle. We believe that this method of presentation of the information provided by our instrument will be of practical utility for the road maintenance community.

4.2 INSTRUMENT CALIBRATION

Calibrations of the sensor system under controlled road surface conditions were performed in CRREL's Frost Effects Research Facility. The test set up is shown in Figure 18. It consists of approximately 20 ft pavement surface on which different ice, snow, wet, and dry conditions were created. The sensor was mounted on a platform that could be traversed both longitudinally along the length of the pavement and laterally across the pavement. During data acquisition, the sensor was swept back and forth at approximately 8 mph for about 10 minutes. The data was sampled at 1 kHz, averaged over several samples and recorded on a PC. During operation of this experiment, we used discrimination software described in the previous reports. Our data acquisition PC was programmed for CRREL calibrations and the same unit and algorithms were used in subsequent road tests at CRREL and Colorado DoT.

Over 40 calibration tests were run at CRREL. The test matrix is included in Appendix B. Figures 19 through 22 show photographs of some of the surface conditions we created at CRREL; namely, wet asphalt with some standing water, moist ice, dry ice, warm packed snow, and, respectively. In this section, we present sensor data collected on these surfaces. Unfortunately, we do not have a photograph of a dry snow surface used in calibrations, but we will show the sensor data for this case as well.

Examples of sensor outputs as the device is traversed back and forth on the above surfaces are shown in Figures 23 through 27. Figure 23 shows data for the surface in Figure 19, wet asphalt with some standing water. Figure 23(a) shows the averaged signals in three wavelength channels, λ_1, λ_2, and λ_3 for 5 cycles (10 strokes back and forth). The data are very repeatable (except for one isolated peak in the fifth cycle). As expected, we see that the absorption at λ_2 wavelength in water is greater than absorption at λ_3. This is reflected in the ratio of intensities at these two wavelengths, to be less than 1, approximately 0.7, as seen in Figure 23(b). It is also seen that the ratio of intensity in the λ_2 channel to the intensity in the λ_1 channel is significantly less than 1, in

fact less than 0.5 in most of the data. This ratio, when less

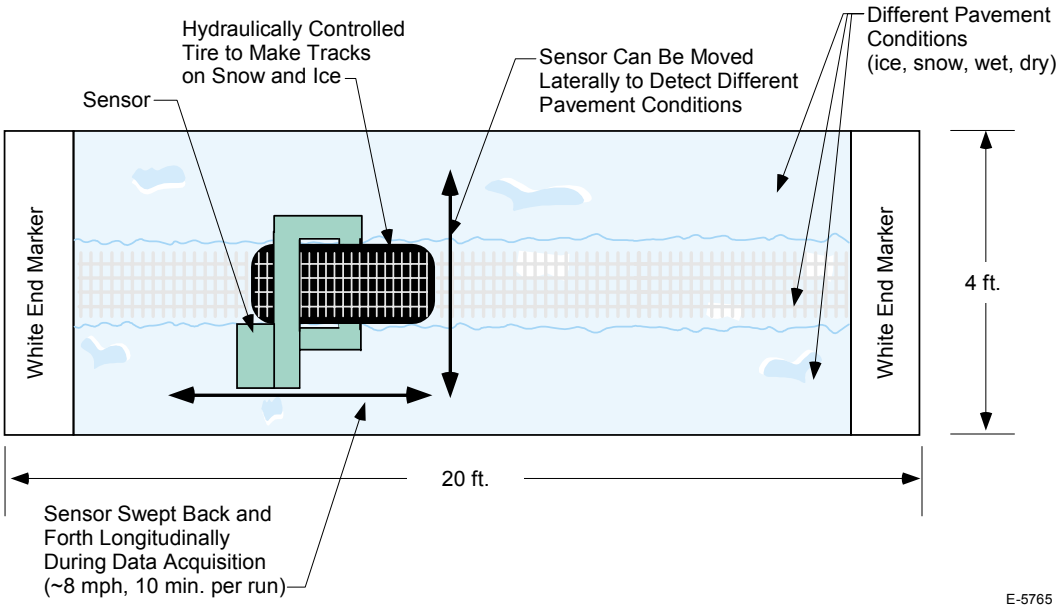

FIGURE 18 CRREL Frost Research Facility test setup.

FIGURE 19 Wet asphalt surface with some standing water.

than 0.5, characterizes the presence of water, as we have discussed earlier in this report. Figure 23(c) shows a map of the ratio of scattered light intensity at λ_2 to intensity at λ_3 plotted against the ratio of intensity at λ_2 to intensity at λ_1. As discussed in Subsection 3.2, this map presents an informative description of the road conditions and it is divided into various surface types based on the laboratory sensor calibrations performed earlier.[2] We see that the CRREL data falls neatly in the regions identified as "water" and "moist". In fact, most points fall in the water region and their trend indicates that the points near the origin are associated with deeper water in the pool.

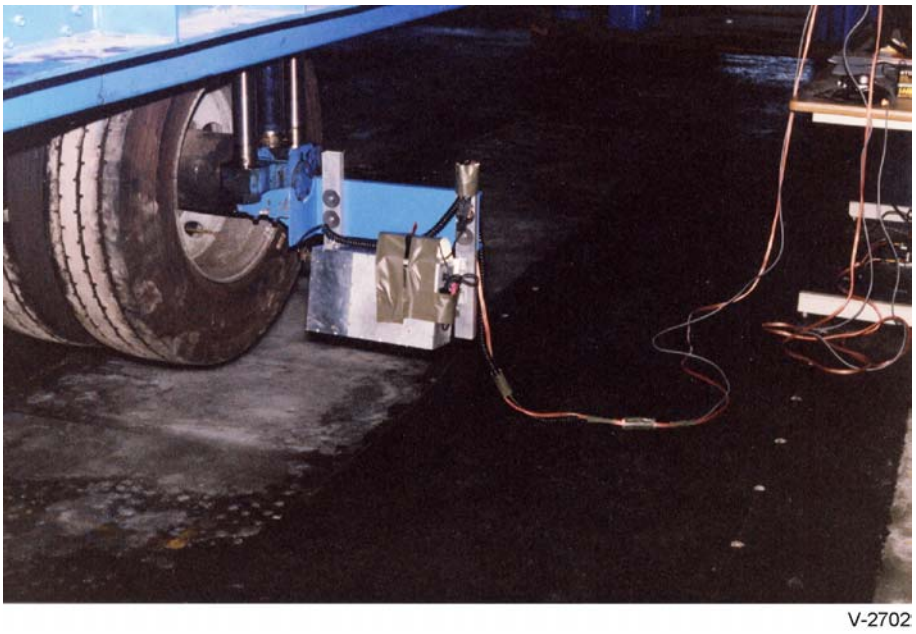

FIGURE 20 Moist icy surface.

FIGURE 21 Dry icy surface.

Figure 24 shows similar data for the moist icy surface shown in Figure 20. Figure 24(a) shows the averaged signals in three wavelength channels, λ_1, λ_2, and λ_3. It is seen the intensities in λ_2 and λ_3 channels are about the same and their ratio (Figure 24(b)) is closer to 1, approximately 0.9. The discrimination map in Figure 24(c) shows that the sensor classified the surface as mostly moist, with a few points characterized as water as well as ice. Thus, the sensor appears to produce sensible characterization of the test surface. We discovered in additional tests that when the water layer on top of ice becomes sufficiently thick the sensor correctly identifies the water but not the ice underneath it. We believe that this limitation can be overcome by selection of slightly different wavelengths from those currently used. Essentially, this would necessitate filters at these modified wavelengths, which is a straightforward modification.

V-2707

FIGURE 22 Warm, packed snow surface.

Figure 25 shows data for a dry icy surface shown in Figure 21. Figure 24(a) shows the averaged signals in three wavelength channels, λ_1, λ_2, and λ_3. It is seen the intensities in λ_2 channel are consistently greater than the intensities in the λ_3 channel by a small amount and their ratio (Figure 25(b)) is greater than 1, approximately 1.1 to 1.2. It is also seen that the ratio of intensity in the λ_2 channel to the intensity in the λ_1 channel is greater than 0.5, in fact it is fairly constant around 0.6 for most of the data. The high value of this ratio indicates absence of water; consistent with the condition of the dry icy surface. The discrimination map in Figure 25(c) shows that the sensor correctly classified the surface as icy, with points clustered closely in that region. Again, the sensor's characterization of the test surface condition agrees with visual observations.

Figure 26 shows data for a surface with warm packed snow (or slush) as shown in Figure 22. Figure 26(a) shows the averaged signals in three wavelength channels, λ_1, λ_2, and λ_3. It is seen the intensities in λ_2 channel are lower than the case of dry icy surface due to absorption in water and the intensities in the λ_3 are lower due to absorption in ice. Furthermore, the signals in the λ_3 channel are much lower than those in the λ_2 channel. As a result, Figure 26(b) shows that the ratio of λ_2 intensity to λ_3 intensity is greater than 2.5. It is also seen that the ratio of intensity in the λ_2 channel to the intensity in the λ_1 channel is less than 0.5, indicating the presence of water. The discrimination map in Figure 26(c) shows that the sensor has correctly classified the surface to be composed of snow, slush (ice and water), and water.

Finally, we discuss calibration data for a dry snow surface (for which a photograph is not available) shown in Figure 27. Figure 27(a) shows the averaged signals in three wavelength channels, λ_1, λ_2, and λ_3. It is seen the intensities in all channels are significantly higher than in all previous cases, particularly, in the λ_1 and λ_2 channels. This is because snow scatters near infrared light very efficiently. As a result, Figure 27(b) shows that the ratio of λ_2 intensity to λ_3 intensity is very high, greater than 4.5. It is also seen that the ratio of intensity in the λ_2 channel to the intensity in the λ_1 channel is greater than 0.5, in fact it is fairly constant around 0.6. The high value of this ratio indicates absence of water; consistent with the condition of the dry snow. The discrimination map in Figure 27(c) shows that the sensor has correctly classified the surface as mostly snow. (We believe that the ice characterization is due to "edge effects" associated with the data points on the rapidly rising and falling portions of the pulses in Figure 27(b)). PSI and CRREL collected and analyzed a large quantity of calibration data on a variety of test surfaces. Selected examples from these data are included in Appendix B of this report.

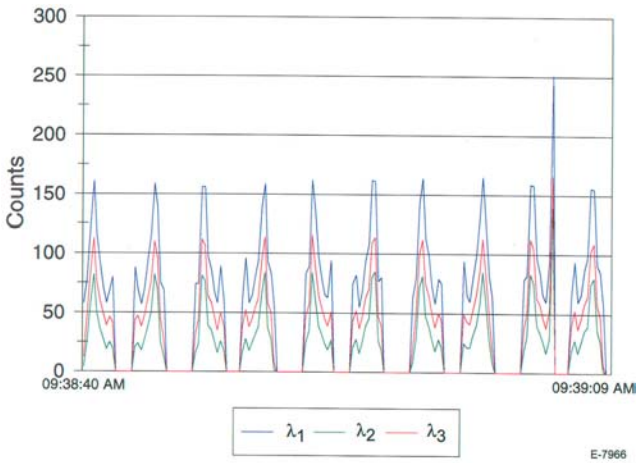

(a) Averaged signals in λ_1, λ_2, and λ_3 channels.

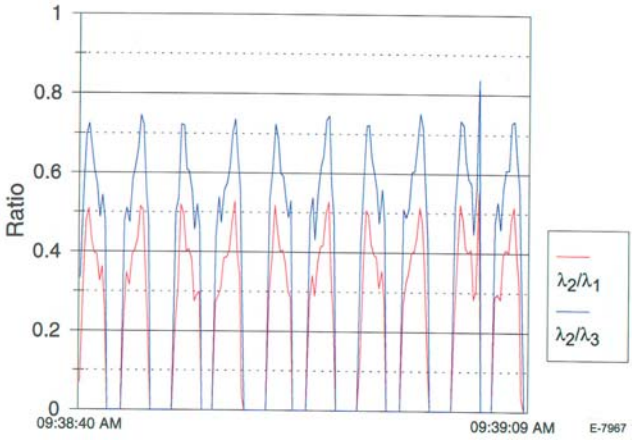

(b) Ratio of intensities in λ_1, λ_2, and λ_3 channels.

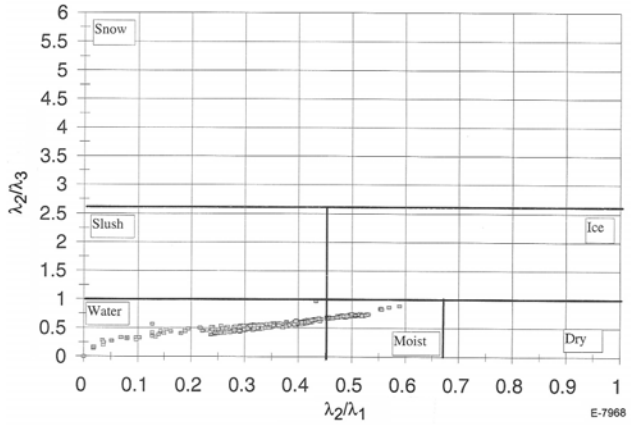

(c) Road condition discrimination map

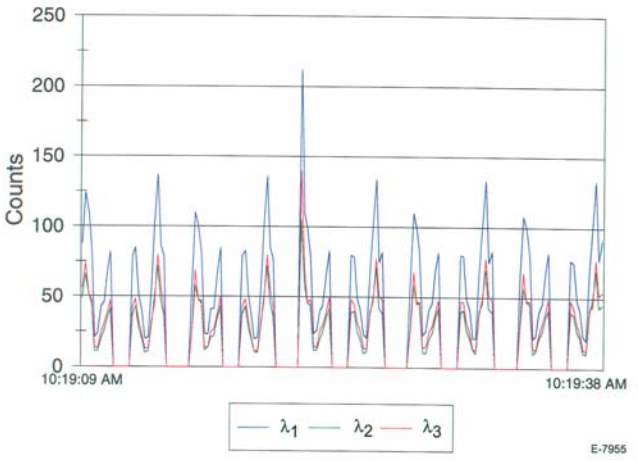

(a) Averaged signals in λ_1, λ_2, and λ_3 channels.

FIGURE 23 Sensor calibration data on a wet asphalt surface with standing water (Figure 19).

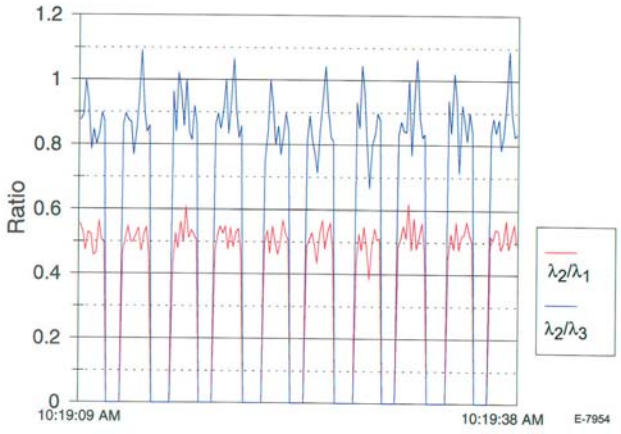

(b) Ratio of intensities in λ_1, λ_2, and λ_3 channels.

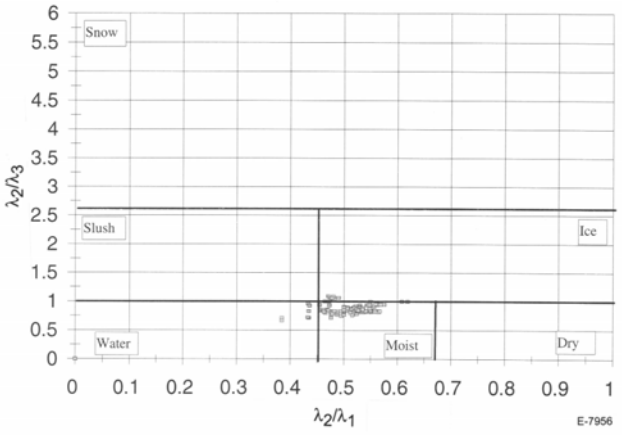

(c) Road condition discrimination map.

FIGURE 24 Sensor calibration data on a moist icy surface (Figure 20).

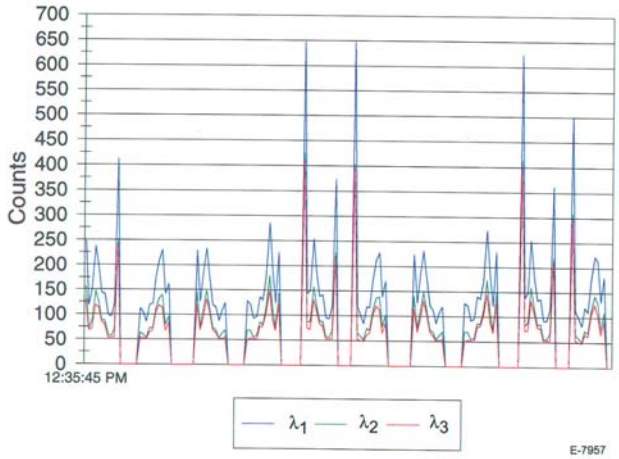

(a) Averaged signals in λ_1, λ_2, and λ_3 channels.

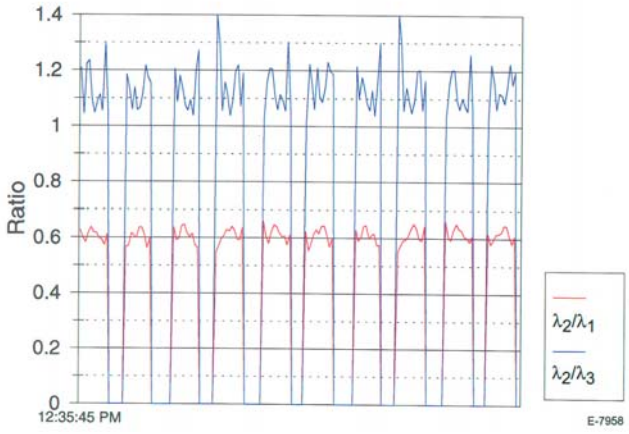

(b) Ratio of intensities in λ_1, λ_2, and λ_3 channels.

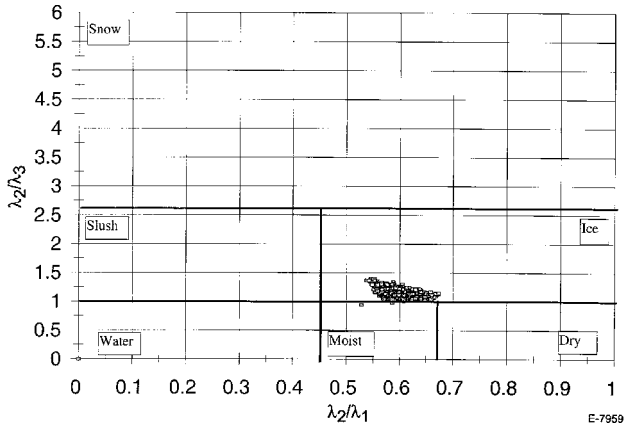

(c) Road condition discrimination map.

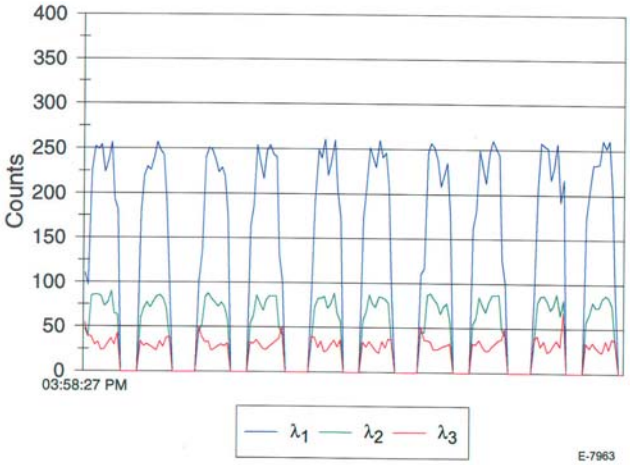

(a) Averaged signals in λ_1, λ_2, and λ_3 channels.

FIGURE 25 Sensor calibration data on a dry icy surface (Figure 21).

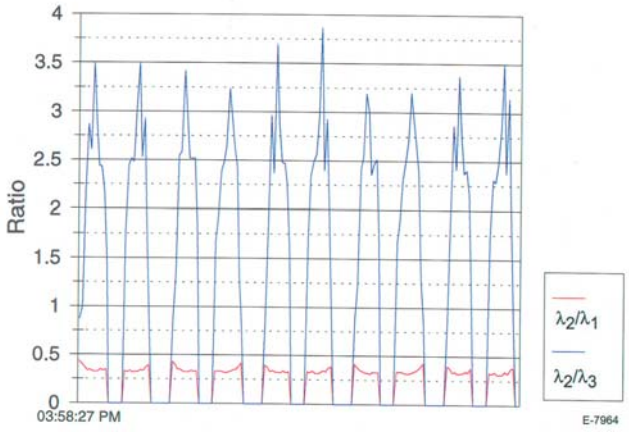

(b) Ratio of intensities in λ_1, λ_2, and λ_3 channels.

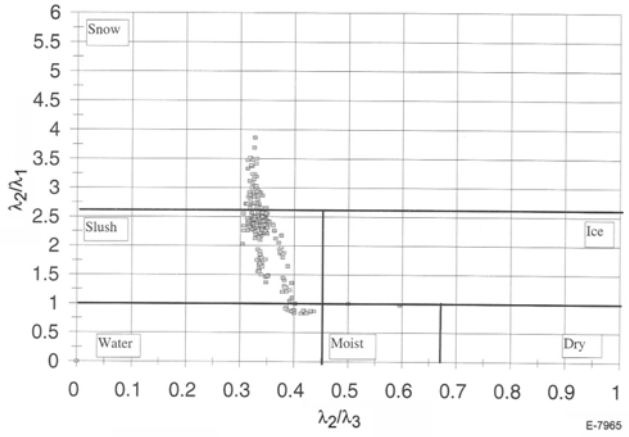

(c) Road condition discrimination map.

FIGURE 26 Sensor calibration data on a surface with a layer of warm, packed snow (Figure 22).

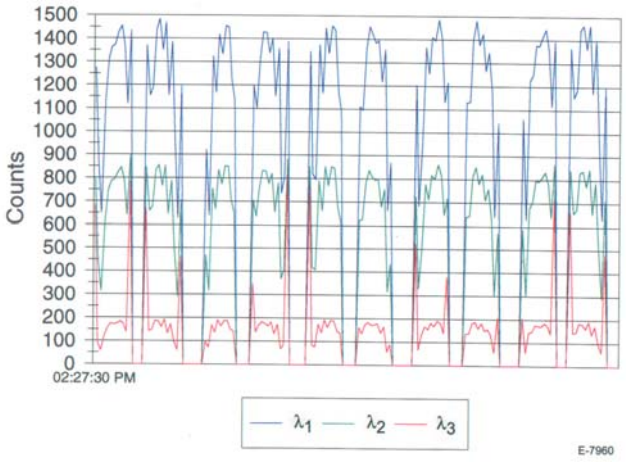

(a) Averaged signals in λ_1, λ_2, and λ_3 channels.

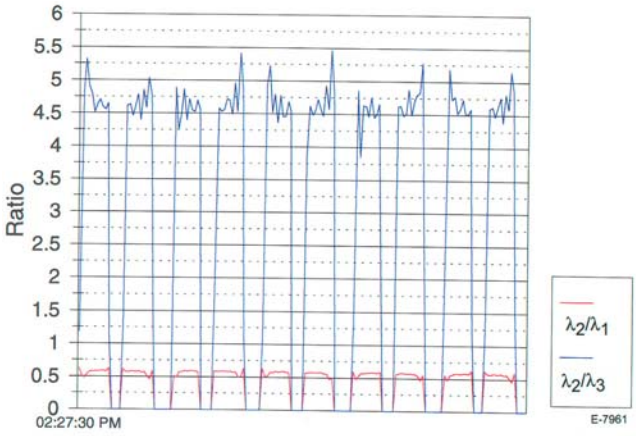

(b) Ratio of intensities in λ_1, λ_2, and λ_3 channels.

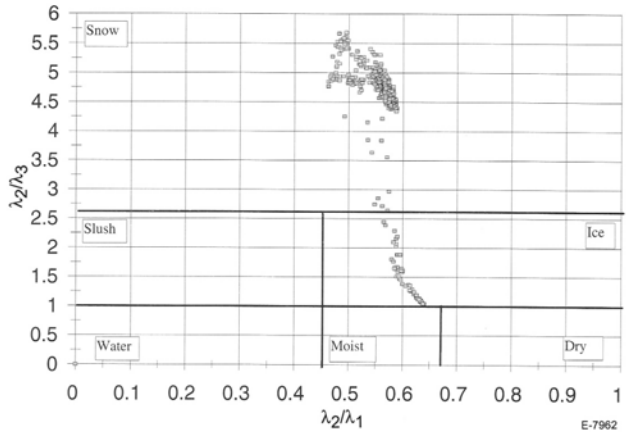

(c) Road condition discrimination map.

FIGURE 27 Sensor calibration data on a surface with a layer of dry snow.

4.3 INSTRUMENT FIELD TESTS

The tests were conducted on roads in the vicinity of CRREL facilities in Hanover, New Hampshire during winter 2000. The sensor was mounted on the front bumper of CRREL's Instrumented Research Vehicle (IRV) as shown in Figure 28. For some runs, the IRV was fitted with a traction device for monitoring the frictional forces between the tires and the road surface, Figure 29. The traction data were analyzed independently by CRREL. A complete matrix of CRREL road tests is included in the Appendix C. We discuss data from selected tests in this report.

Figure 30 shows a road surface that was described visually by the IRV operator as pavement with dry and moist regions. Data was collected at 1 kHz sampling rate as in calibration tests. The test data is contained in Figure 31. The time series of averaged sensor outputs in λ_1, λ_2, and λ_3 wavelength channels are shown in Figure 31(a). The signals also exhibit significant high frequency content on the roadway compared to the calibration data under controlled conditions (see Appendix B). Note that the intensity at λ_2 is lower than that in the other two channels, indicating absorption due to the presence of water. The ratios of intensities in the λ_2 and λ_3 channels and intensities in the λ_2 and λ_1 channels are shown in Figure 31(b). The λ_2 to λ_3 ratio is less than 1 indicating either a dry or moist (wet) pavement, and the λ_2 to λ_1 ratio is greater than 0.5 indicating a moist pavement. This trend is reflected in the discrimination map of Figure 31(c) where the ratio of intensity in λ_2 channel to the intensity in λ_3 channel is plotted against the ratio of intensity in the λ_2 channel to the intensity in λ_1 channel. The sensor characterizes the pavement over which the IRV was driven as moist (wet) and dry, consistent with the operator's observations. Further, the sensor indicates that the wet regions were more predominant than the dry regions.

Next, we show data verifying sensor operation on a roadway covered with mostly packed snow, as shown in Figure 32. The averaged sensor outputs in λ_1, λ_2, and λ_3 wavelength channels are shown in Figure 33(a). As we saw in the indoor calibration tests at CRREL's Frost Research Facility (reported in Letter Report 1), all channels show significant increase in intensity due to high scattering from the snow. The signals also exhibit lot of fluctuations in intensities, as one would expect on real snowy roadways. On the intensity ratio plot, Figure 33(b), the λ_2-to-λ_3 ratio is very high, greater than 5, for the most part. The ratios are punctuated by higher intensity and lower intensity spikes. The λ_2-to-λ_1 intensity ratio, on the

V-2529

V-2530

FIGURE 28 Sensor mounted on CRREL Instrumented Research Vehicle.

V-2536

V-2537

FIGURE 29 CRREL IRV with traction monitoring device and road condition sensor.

other hand, is remarkably flat with a value of about 0.6, indicating absence of water. The discrimination map in Figure 33(c) shows that the sensor indeed characterizes the road surface as almost completely snow, thus validating its operation on that surface

We now consider the case of sensor operation over a complex pavement characterized visually by the operator as a combination of thawing soil, snow, and ice. (Unfortunately, photograph of this surface is not available.) The averaged sensor outputs in λ_1, λ_2, and λ_3 wavelength channels are shown in Figure 34(a). The λ_1 and λ_2 signals are quite

FIGURE 30 Photograph of pavement with dry and moist regions.

high (indicating snow) and display substantial fluctuations in intensities. There are two regions, however, where the intensities drop significantly, with the λ_2 and λ_3 signals about equal indicating presence of water/moisture. In Figure 34(b), the λ_2-to-λ_3 intensity ratio is mostly greater than 2, indicating snowy regions. This ratio also has areas where its value is around 1 or less than 1, indicating icy or wet regions. We also note that the λ_2-to-λ_1 intensity ratio is relatively flat with a value of about 0.5, indicating possibly wet regions. The discrimination map in Figure 34(c) shows that the sensor characterizes the road as having many types of surface layers. These include large snow regions, as well as slushy and wet portions, and even water films in some places. This description agrees with the operator's qualitative observations. We conclude therefore that our sensor characterizes winter road surface conditions accurately.

The sensor then was shipped to the Colorado Department of Transportation for trials during winter 2001. This test series was concluded successfully, with the CoDoT personnel's observation that the sensor worked very well. A large quantity of data from these tests was collected but we have not been able to analyze it in detail due to resource limitations. PSI is pursuing other government agencies for funding to analyze these data and also to make hardware modifications to the engineering prototype instrument.

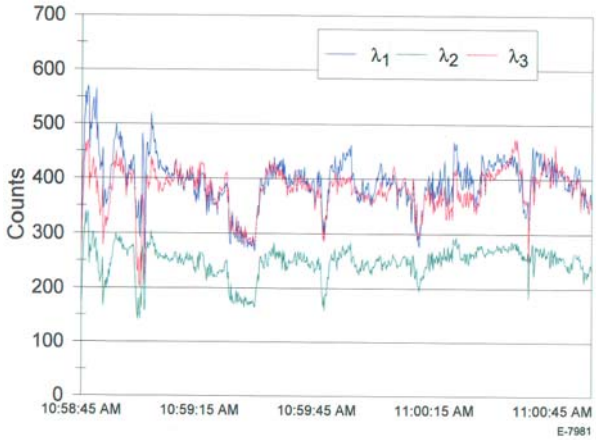

(a) Averaged sensor signals in outputs in λ_1, λ_2, and λ_3 wavelength channels.

(b) Ratio of intensities in λ_2 and λ_3 channels and ratio of intensities in λ_2 and λ_1 channels.

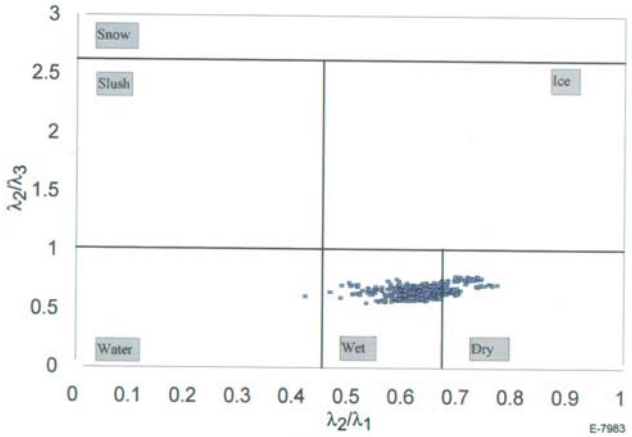

(c) Pavement condition discrimination map: Ratio of intensity in λ_2 channel to intensity in λ_3 channel is plotted against the ratio of intensity in λ_2 channel to intensity in λ_1 channel.

FIGURE 31 Sensor data from CRREL IRV road test over dry pavement with moist patches.

V-2533

V-2698

FIGURE 32 Sensor operation verification on a snow covered pavement.

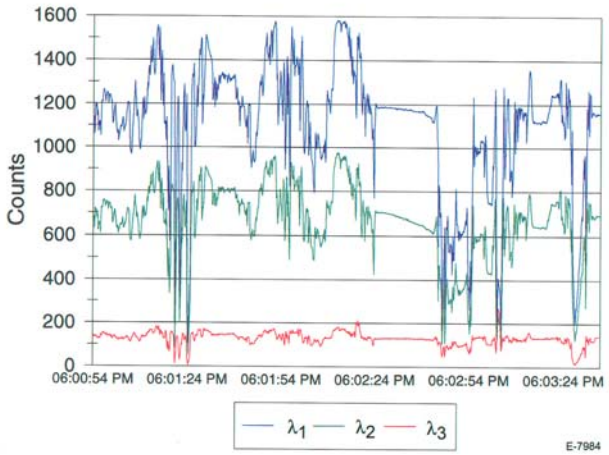

(a) Averaged sensor signals in outputs in λ_1, λ_2, and λ_3 wavelength channels.

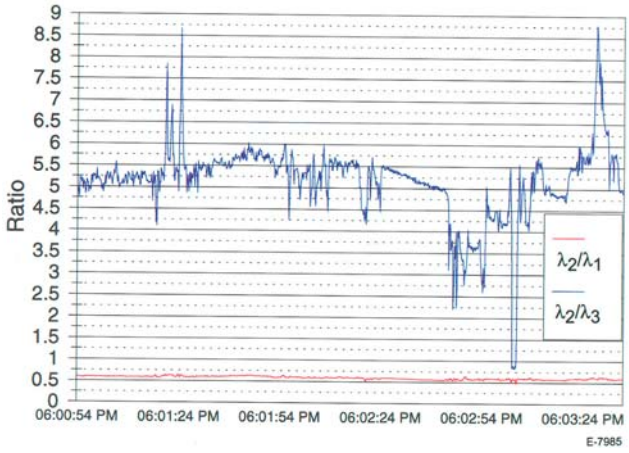

(b) Ratio of intensities in λ_2 and λ_3 channels and ratio of intensities in λ_2 and λ_1 channels.

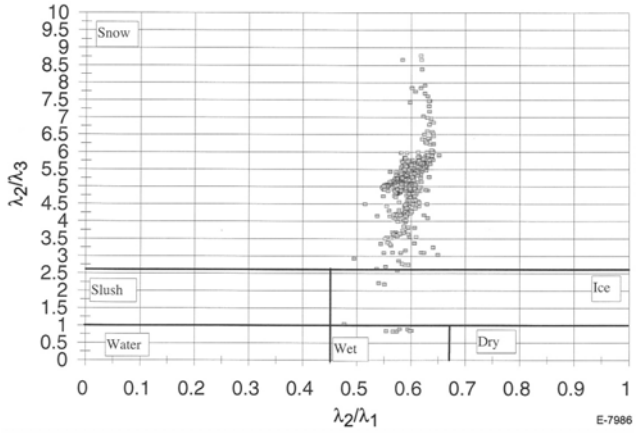

(c) Pavement condition discrimination map: Ratio of intensity in λ_2 channel to intensity in λ_3 channel is plotted against the ratio of intensity in λ_2 channel to intensity in λ_1 channel.

FIGURE 33 Sensor data from CRREL IRV road test over snow-covered pavement.

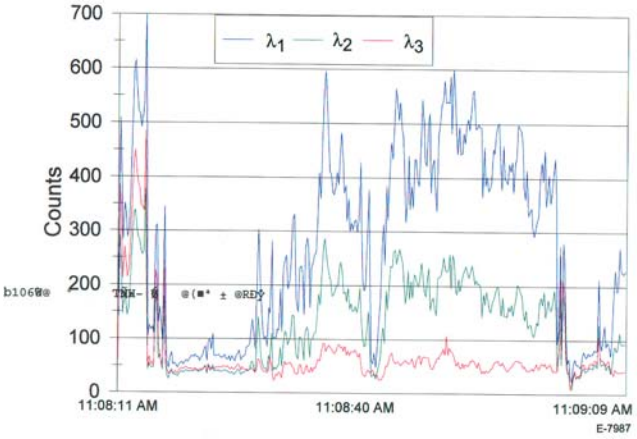

(a) Averaged sensor signals in outputs in λ_1, λ_2, and λ_3 wavelength channels**.**

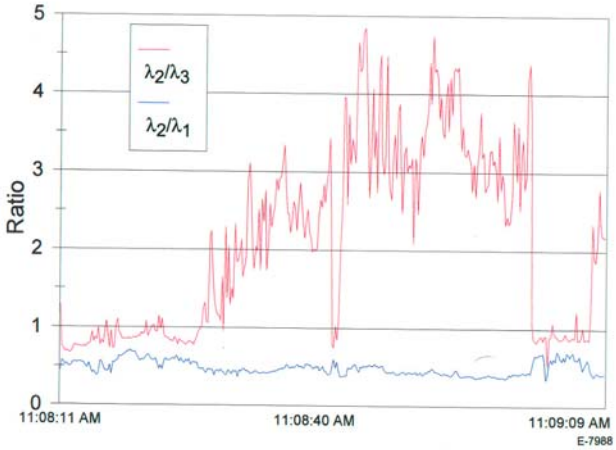

(b) Ratio of intensities in λ_2 and λ_3 channels and ratio of intensities in λ_2 and λ_1 channels.

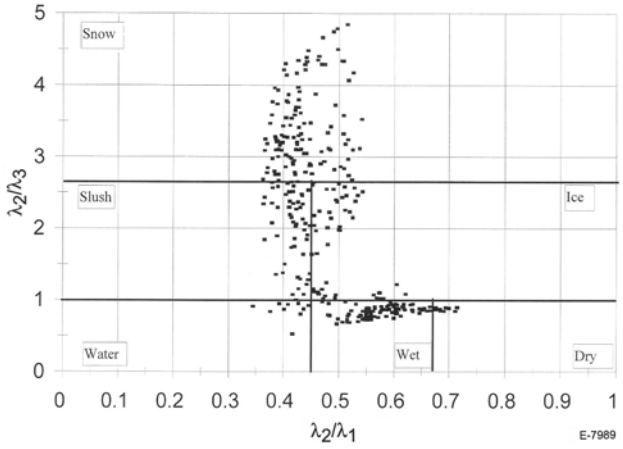

(c) Pavement condition discrimination map: Ratio of intensity in λ_2 channel to intensity in λ_3 channel is plotted against the ratio of intensity in λ_2 channel to intensity in λ_1 channel.

FIGURE 34 Sensor data from CRREL IRV road test over pavement consisting of thawing soil, snow, and ice.

5. SUMMARY OF RESULTS AND RECOMMENDATIONS

The results of this ITS-85 IDEA program are summarized below.

1. A mobile, vehicle-mounted sensor system for detection and monitoring of winter road conditions was developed. An engineering prototype of the system was built, calibrated, and successfully road-tested under winter climate. The calibration and field tests clearly demonstrated the ability of the sensor system to discriminate among various winter road conditions such as thin films of ice and water, wet and dry pavement, water-covered, sand-covered and snow-covered pavement surfaces as well as complex combinations of these surface conditions.

2. The sensor system performed the road condition discrimination in real time and displayed the information in an easy to follow, continually updated graphical format on a PC for the vehicle operator. The data were also stored for subsequent detailed analysis.

3. The instrument was carefully calibrated at the CRREL Frost Research Facility by creating controlled surface conditions (ice, water, dry, moist, sand, dry snow, wet snow, etc.) and comparing those to the sensor system indications. Winter road testing was successfully performed on the CRREL Instrumented Research Vehicle, a Massachusetts Highway Department maintenance truck, and a Colorado DoT winter maintenance vehicle. In all tests, the road conditions as described by a human observer agreed well with the conditions indicated by the prototype instrument.

4. The prototype sensor system was evaluated by Surface Systems Inc. of St. Louis in the laboratory as a candidate system for commercial winter maintenance vehicles. The sensor worked as predictably in this evaluation. They have recommended further testing under the auspices of state departments of transportation.

We recommend the following modifications and improvements to optimize the sensor system for future commercial applications.

1. Adjust filter wavelengths to enable more accurate discrimination of ice under a thin layer of water. This can be achieved without increase in cost of the system.

2. Implement 1 mm diameter detectors, instead of the current 3 mm diameter design, to reduce cost of the system.

3. Incorporate a silicon photodiode (which was envisaged in the current design) in the shortest wavelength channel to correct for the effects of solar reflections from pavement surfaces and modify discrimination algorithms accordingly. This would have negligible impact on the sensor cost, but the discrimination among dry, moist, and wet surfaces would be markedly improved.

4. Analyze data from Colorado DoT field tests and the remaining data form CRREL field tests. Incorporate results to validate and, if necessary, modify the discrimination algorithms.

5. Continue further field testing with state departments of transportation and U.S. Army components, and continue to seek commercialization opportunities.

REFERENCES

1. Emerging Concepts and Products for Intelligent Transportation Systems, Transportation Research Board, IVHS-IDEA Program, September 1994.

2. Joshi, P. B., Rosen, D. I., Fike, E. E., Malonson, M. R., and Lund, E. J., "Road Surface Condition Detection and Monitoring Technology for a Vehicle-mounted Hazard Warning System," Type I Concept Exploration Project Final Report, National Academy of Sciences Contract No. ITS-50, Physical Sciences Inc. Technical Report PSI-2446/TR-1574, September 1998.

3. Rosen, D., "Investigations of Active Infrared Detection of Pavement Icing," Final Contract Report to U.S. Army Cold Regions Research and Engineering Laboratory, Hanover, NH, contract No. DACA33-86-C-0015, PSI-2013/TR-655, March 1998.

4. Pavement and Bridge Icing, Transportation Research Board, National Research Council, Transportation Research Record #576, 1976.

5. Meyer, W. et al., "Bridge Deck Deicing Study, Penn State University Report TTSC 7014, August 1970.